

**Prebiotic-Chemistry Inspired Polymeric Coatings for the
Surface Modification of Hydrophobic Polyethersulfone
membranes for the Enhancement of their Antifouling and
Antibacterial Properties**

By

Shruti Srinivas

A thesis submitted in partial fulfillment of the requirements for
the degree of

Master of Science

In

Chemical Engineering

Department of Chemical and Materials Engineering

University of Alberta

© **Shruti Srinivas, 2020**

Abstract

Polyethersulfone (PES) membranes are very commonly used for wastewater treatment because of their excellent mechanical, chemical and thermal properties. However, the major concern associated with these membranes is their susceptibility to fouling due to their intrinsic hydrophobicity. Therefore, in this study, we demonstrate a new and facile surface modification technique using the prebiotic-chemistry inspired approach, to enhance the hydrophilicity and antifouling properties of the PES membrane. Prebiotic chemistry is the study of molecules and reactions that led to the origin of life on earth and the most commonly studied polymers in the field of prebiotic chemistry are the hydrogen cyanide (HCN) derived polymers.

The surface modification of the PES membrane was first obtained using aminomalonitrile (AMN), a trimer of hydrogen cyanide followed by the sequential deposition of two different polymers, a hydrophilic glycopolymer (poly(2- lactobionamidoethyl methacrylamide) P(LAEMA) and a zwitterionic polymer (poly(sulfobetaine methacrylate)) P(SBMA) to render the surface of the PES membrane hydrophilic. Surface characterizations were carried out using X-ray photoelectron spectroscopy (XPS), and Attenuated total reflectance Fourier transform infrared (ATR-FTIR) spectroscopy to confirm the successful modification of the PES membrane surface using AMN and the deposition of polymers P(LAEMA) and P(SBMA). The Atomic force microscopy (AFM) measurements were carried out to determine the surface roughness of the modified membranes, the water contact angle measurement (WCA) were performed to determine the hydrophilicity of the membrane surface. The static protein adsorption tests were performed using bovine serum albumin (BSA) as a model protein to determine the antifouling ability of the membranes surface before and after its modification. Further, the surface morphology of the membranes after their immersion into BSA was determined using the scanning electron microscopy (SEM).

Furthermore, silver nanoparticles (Ag NPs) were deposited onto the surface of the modified membranes without the need for any reducing agents. The membranes were then tested for their antibacterial ability.

Acknowledgements

Firstly, I would like to thank my supervisors Dr. Hongbo Zeng and Dr. Ravin Narain for their excellent guidance, encouragement, support and patience during the entire two years of my Masters' study and research at the University of Alberta. Their guidance throughout my research helped me gain both practical and theoretical knowledge related to my project. The immense support I have received from them during the two years of my study has moulded me into the person I am today and has taught me to think out of the box and has also given me the confidence to perform individual research.

Secondly, I would like to thank my thesis committee members for agreeing to be a part of my committee and for their thoughtful comments, suggestions and words of encouragement regarding my research. The thought-provoking conversations I had with my committee regarding my research has helped me think deeply and widen my research perspective. I would also like to thank my graduate coordinator Dr. Vinay Prasad for believing in me and for his immense guidance that helped me smoothly finish my thesis.

Thirdly, I would like to thank both my friends and labmates for their moral support and guidance and for all the timely help I had received from them since the day I began my studies at this prestigious institution. I had a lot of fun working with each and every one of them and connecting with them on a personal level. I would especially like to thank my colleague Yi-Yang Peng (Kevin) for his patience, support and guidance since the day I began my research.

Last but not the least I would like to thank my family; (1) my father and mother for the continuous moral support they had provided me with, for motivating and pushing me to believe in myself during the tough times and for never allowing me to give up. I am forever indebted to them for providing me with the opportunities that have shaped me into the person I am today, (2) my brother for always being my best friend, and for making me laugh with his witty sense of humor to get me going through the tough times, (3) Rahul, for his immense patience and support, for never letting me give up and for all the help I received from him in terms of both coursework and research work.

Table of Contents

LAYOUT OF THE THESIS	xiii
CHAPTER 1: BACKGROUND	1
1.1. Introduction.....	1
1.2. Membrane Technology	1
1.2.1. Membrane Fouling and Surface Modification	2
1.3. Antifouling Materials for Surface Modification.....	4
1.3.1. Mussel-Inspired Surface Chemistry for Surface Modification	6
1.4. Prebiotic-Chemistry Inspired Surface Modification Approach.....	7
1.5. Research Objective	10
CHAPTER 2: POLYMERIZATION AND CHARACTERIZATION TECHNIQUES	12
2.1. Polymerization Techniques.....	12
2.1.1. Living or Controlled Radical Polymerization (CRP)	12
2.1.1.1. Reversible Addition-Fragmentation Chain Transfer (RAFT) Mechanism	12
2.2. Characterization Techniques.....	14
2.2.1. Nuclear Magnetic Resonance Spectroscopy (NMR).....	14
2.2.2. Atomic Force Microscopy (AFM).....	16
2.2.3. X-ray Photoelectron Spectroscopy (XPS).....	19
2.2.4. Scanning Electron Microscopy (SEM).....	19
2.2.5. Water Contact Angle Measurements	21
2.2.6. Ultraviolet–Visible (UV-Vis) Spectroscopy	22
CHAPTER 3: PREBIOTIC-CHEMISTRY INSPIRED POLYMERIC COATINGS OF POLYETHERSULFONE (PES) ULTRAFILTRATION MEMBRANES FOR ENHANCED ANTIFOULING AND ANTIBACTERIAL PROPERTIES	24
3.1. Introduction.....	24

3.2. Experimental.....	29
3.2.1. Materials	29
3.2.2. Methods	30
3.2.2.1. Polymer Synthesis and Characterization.....	30
3.2.2.2. Membrane Pre-treatment and Surface Modification.....	31
3.2.2.3. Membrane Surface Characterizations	32
3.2.2.4. Static Protein Adsorption Tests.....	33
3.2.2.5. Antibacterial Studies	34
3.3. Results and Discussion	34
3.3.1. Polymer Synthesis and Characterization.....	34
3.3.2. Surface Chemical Composition of the Membranes	37
3.3.3. Surface Wettability and Roughness of the Membranes	40
3.3.4. Static Protein Adsorption tests	43
3.3.5. Surface Morphology of the Membranes after Fouling	45
3.3.6. Antibacterial Activity of the Membranes.....	46
CHAPTER 4: CONCLUSION AND FUTURE WORK	50
BIBLIOGRAPHY	52

List of Tables

Table 3.1: A summary of the previous surface modification strategies

Table 3.2: Surface elemental composition of AgNPs on membrane surfaces

Table 3.3: Contact angle and surface roughness parameters of the membranes

List of Figures

Figure 1.1: Separation process using membranes.

Figure 1.2: Schematic view of the fouling process in membranes. Figure adapted from [15].

Figure 1.3: Chain hydration mechanism for hydrophilic and zwitterionic polymers. Figure adapted from [33].

Figure 1.4: Surface modification of filtration membranes via direct coating and grafting of polymeric chains. Figure adapted from [34].

Figure 1.5: The apparatus used for the spark for the experiment. Figure reproduced with permission from [40].

Figure 1.6: Structure of aminomalonitrile (AMN). Figure adapted from [41].

Figure 1.7: The simple one-step procedure of aminomalonitrile (AMN)-based coatings. Figure reproduced with permission from [42].

Figure 2.1: Schematics of the working principle of AFM. Figure reproduced with permission from [51].

Figure 2.2: The schematic representation of a scanning electron microscope. Figure reproduced with permission from [59].

Figure 2.3: Water contact angle measurement on a solid surface. Figure reproduced with permission from [61].

Figure 3.1: Chemical structures of polyethersulfone (A) and aminomalonitrile p-toluenesulfonate (B). Figure (B) adapted from [81].

Figure 3.2: Schematic representation of the prebiotic-chemistry inspired polymeric coating.

Figure 3.3: Chemical structures of ACVA and CTP.

Figure 3.4: The schematic representation of the RAFT polymerization mechanism.

Figure 3.5: Schematic representation of pre-treatment of filtration membranes.

Figure 3.6: Schematic representation of the membrane coating process.

Figure 3.7: Schematic representation of the static protein adsorption steps; (Step 1) membrane preparation for fouling tests, (Step 2) BCA assay protocol for quantifying the protein content.

Figure 3.8 (a): ^1H NMR spectra of P(LAEMA) in D_2O .

Figure 3.8 (b): ^1H NMR spectra of P(SBMA) in D_2O .

Figure 3.9: XPS spectra of the modified and unmodified membranes.

Figure 3.10: EDX images of the modified and unmodified membranes deposited with AgNPs.

Figure 3.11: Static water contact angle measurements of the modified and unmodified membranes.

Figure 3.12: Two-dimensional topographical AFM images of the modified and unmodified membranes.

Figure 3.13: Static protein adhesion tests on the modified and unmodified membrane surfaces.

Figure 3.14: SEM images of the modified and unmodified membranes after fouling with BSA.

Figure 3.15 (a): Inhibition zone images of both modified and unmodified membranes against gram negative (*E. coli*) before and after their incorporation with AgNPs.

Figure 3.15 (b): Inhibition zone images of both modified and unmodified membranes against gram positive (*S. aureus*) before and after their incorporation with AgNPs.

Scheme 2.1: Kinetics of RAFT polymerization technique. Scheme adapted from [47].

List of Abbreviations

AFM: Atomic Force Microscopy

AMN: Aminomalonitrile

ATR-FTIR: Attenuated Total Reflection- Fourier Transform Infrared Spectra

BSA: Bovine Serum Albumin

CW: Continuous Wave

CTA: Chain Transfer Agent

CTP: Cyanopentanoic Acid Dithiobenzoate

DMF: *N,N'*-dimethylformamide

DOPA: 3,4-Dihydroxyphenylalanine

DHBA: 3,4-di- benzaldehyde

ESBD: Electron Backscatter Diffraction

E.coli: Escherichia coli

FRP: Free Radical Polymerization

FO: Forward Osmosis

FT: Fourier Transform

HCN: Hydrogen Cyanide

HSCs: Human Mesenchymal Stem Cells

HCMUs: Hydrogen Cyanide Monomeric Unit

IR: Infrared

LAEMA: Lactobionamidoethyl Methacrylamide

LB: Luria-Bertani Broth

M_n : Number Average Molecular Weight

M_w: Weight Average Molecular Weight

MCWO: Molecular Weight Cut-Off

MF: Microfiltration

NF: Nanofiltration

NMR: Nuclear Magnetic Resonance Spectroscopy

NOM: Natural Organic Matter

PBS: Phosphate Buffer Saline

PSPD: Position Sensitive Photodetector

PDI: Polydispersity Indices

PDOPA: Poly(dopamine)

PES: Polyethersulfone

RAFT: Reversible Addition-Fragmentation Chain Transfer Polymerization

RO: Reverse Osmosis

SPM: Scanning Probe Microscopy

SEM: Scanning Electron Microscopy

SBMA: Sulfobetaine Methacrylate

T_g: Glass Transition Temperature

TCPS: Tissue Culture Polystyrene Surfaces

THBA: 3,4,5-trihydroxy benzaldehyde

THF: Tetrahydrofuran

TS: Tryptic Soy Broth

UF: Ultrafiltration

UV-Vis spec: UV-Vis Spectrophotometer

V_h: Hydrodynamic Volume

Ve: Elution Volume

WCA: Water Contact Angle

XPS: X-Ray Photoelectron Spectroscopy

LAYOUT OF THE THESIS

The thesis comprises four chapters:

Chapter 1 focuses on the concept of membrane technology, the importance of membrane surface modification, the various surface modification approaches, the properties of hydrophilic and zwitterionic polymers, and the prebiotic-chemistry inspired surface chemistry for the surface modification of polyethersulfone (PES) membranes.

Chapter 2 focuses on the kinetics of controlled polymerization technique, particularly focussing on the Reversible Addition-Fragmentation Chain Transfer Polymerization (RAFT) polymerization technique used to synthesize the hydrophilic and zwitterionic polymers. The working principles of the characterization techniques used to characterize the surfaces of the modified PES membranes. The chemical structure of the synthesized polymers is confirmed using the nuclear magnetic resonance spectroscopy (NMR). The X-Ray Photoelectron Spectroscopy (XPS) is used to evaluate the surface chemistry of the modified membranes and the atomic force microscopy (AFM) is used to evaluate their surface roughness. The surface morphology of the polymeric membranes is evaluated using Scanning electron microscopy (SEM). The absorbance of protein solution was determined using a (UV-Vis) spectrophotometer. The surface wettability of the membranes is evaluated using water contact angle measurements (WCA).

Chapter 3 presents the findings of the detailed study of the prebiotic-chemistry inspired polymeric coating approach on pristine polyethersulfone (PES) ultrafiltration membranes to enhance their antifouling and antibacterial properties. The surface modification of the pristine PES membrane was achieved using aminomalonnitrile (AMN), a trimer of hydrogen cyanide. The change in the color of the membrane surface demonstrates the efficient modification of the surface of the PES membrane with AMN. The antifouling ability of the membrane surfaces were evaluated using bovine serum albumin (BSA) as a model protein. The WCA measurements demonstrated enhanced hydrophilicity of the membrane surfaces after their modification with P(LAEMA) and P(SBMA). The modified membranes were further incorporated with silver nanoparticles (AgNPs) and their antibacterial activity against Gram-

negative Escherichia coli (E.coli) and Gram-positive Staphylococcus aureus (S.aureus) bacterial strains was evaluated.

Chapter 4 summarizes the research findings of the current study and will elaborate on the future directions and experiments that could be performed to evolve the environmental applications of the prebiotic-chemistry inspired surface modification approach. This would also help us in achieving a more detailed study and a deeper understanding of the novel surface modification approach in the field of membrane technology.

CHAPTER 1: BACKGROUND

1.1. Introduction

A key solution to the increasing demand for clean water is wastewater reuse and seawater desalination. Though water is the world's most abundant resource, about 1.2 billion people lack access to safe drinking water worldwide. The shortage in water has negatively impacted the continuous economic growth of both developing and industrialized countries and has also hampered both energy and food production. Many wastewater treatment technologies such as physical, chemical and biological treatment technologies have been developed for effectively removing contaminants from wastewater and making water potable and reusable. However, these technologies require complex equipment, consume high energy and are expensive. Some technologies also require a large amount of chemicals for wastewater treatment which result in the generation of chemical by-products. Hence there is a need for the development of cost-effective, robust and energy efficient technology for the efficient purification of wastewater [1-4].

1.2. Membrane Technology

Membrane technology is a separation technology that involves the use of separation membranes for advanced wastewater treatment. The separation membranes used for this technology consume very less energy while removing molecular level contaminants from wastewater. Over the past 50 years, membrane processes are being used in a variety of industrial applications such as (i) water and dairy industry, (ii) biotechnology, (iii) food and beverage industry, (iv) pulp and paper industry, and (v) textile industry and have played a major role in benefitting human life. The separation process involves semi-permeable membranes that act as filters and allow water to flow through them while the suspended solids and other substances present in the water are trapped by the membrane [5, 6].

Polymers are most commonly used for the preparation of filtration membranes as they are less expensive and easier to handle when compared inorganic materials such as ceramics and

metals. Also, membranes fabricated with ceramics are more prone to breakage when compared to polymeric membranes [7, 8]. Various polymeric membranes with different separation mechanisms have been developed and these membranes classified into microfiltration (MF), ultrafiltration (UF), nanofiltration (NF), forward and reverse osmosis (FO & RO) membranes. The factors responsible for the different membrane classifications are: (i) pore sizes, (ii) molecular weight cut-off (MCWO), (iii) transmembrane pressure, and (iv) molecular size of the suspended particles [2, 9]. The schematic representation of the separation process using membranes is shown in **Figure 1.1**. However, one of the serious disadvantages associated with these pressure driven filtration membranes is membrane fouling.

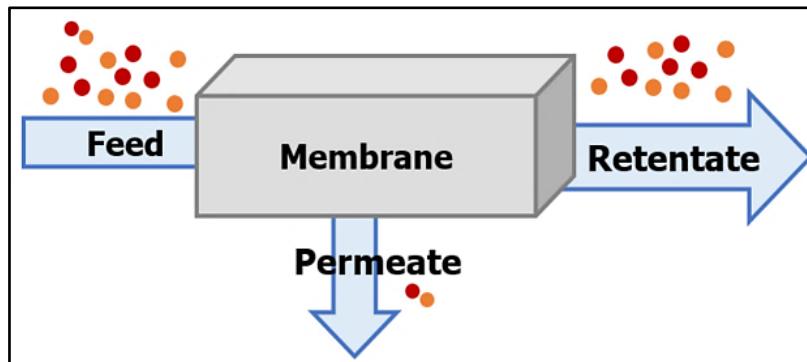


Figure 1.1. Separation process using membranes.

1.2.1. Membrane Fouling and Surface Modification

Fouling in membranes is as a result of the interaction between the surface of the membrane and the substances in the feed water thereby resulting in the deterioration the membrane's performance and lifespan [10, 11]. The feed water consists of natural organic matter (NOM) such as proteins, carbohydrates and microorganisms and they adsorb onto the membrane surface as a result of hydrophobic interactions, hydrogen bonding, van der Waals attractions and electrostatic interactions. This results in the degradation of the membrane material, higher operational costs and a decline in the efficiency of the membranes. The membrane surface characteristics such as surface charge, roughness and hydrophobicity determine the interaction between the foulants present in the feed solution and the membrane surface and are also responsible for membrane fouling [12-15]. The schematic view of membrane fouling process is shown in **Figure 1.2**.

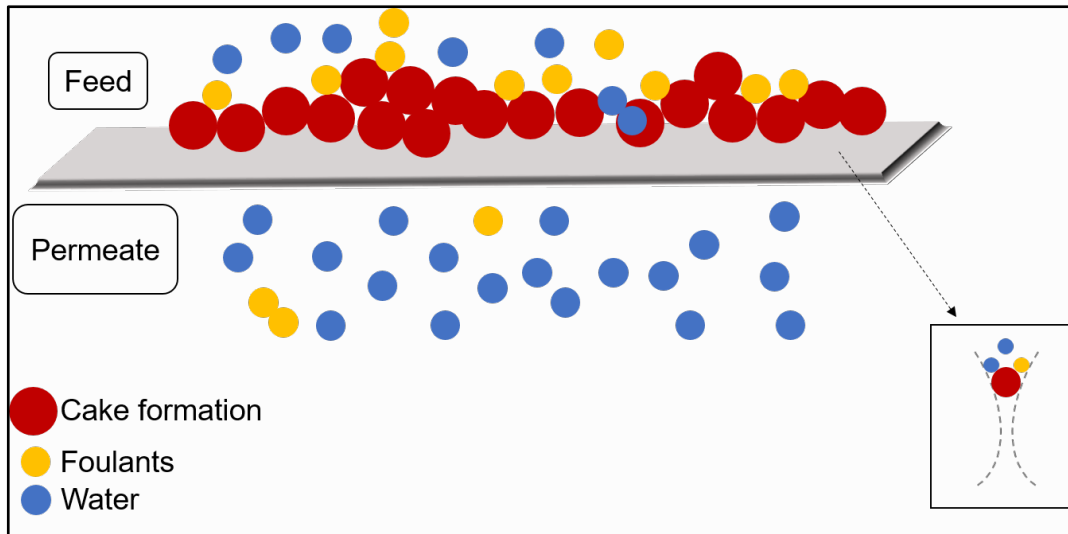


Figure 1.2. Schematic view of the fouling process in membranes. Figure adapted from [16].

Fouling in filtration membranes can be prevented by various pre-treatment processes such as coagulation pretreatment [16], ozone pretreatment [17], adsorption pretreatment [18], and/or by chemical backwashing [19, 20]. However, these methods have their own limitations such as decreasing the life span of the membrane by aggressive washing with chemicals and are higher in costs. Hence hydrophilic surface modification of the membrane is considered to be a facile cost effective strategy to prevent or reduce fouling in filtration membranes. Membrane surface modification is a strategy that aims to reduce or prevent membrane fouling by considering the importance of the surface characteristics of the membrane in regards to fouling. The surface modification strategy involves the introduction of surface charges, hydrophilic groups and smoothing of the membrane surface to minimize the interactions between the foulants and the membrane surface. The intrinsic hydrophobicity of the membrane surface is one of the main reasons for membrane fouling and it has been proven that surface hydrophilization of the membrane surface enhances the antifouling properties of the membrane. Hydrophilic surfaces tend to attract a lot of water molecules thereby reducing protein adsorption on their surfaces and in some cases, they also prevent adsorption [12, 21]. Many physical and chemical surface modification methods such as UV-assisted grafting [22, 23], bulk surface modification [24, 25, 26], Langmuir-Blodgett deposition [27], blending techniques [28], and layer-by-layer assembly [29], have been reported to improve the hydrophilicity of the membrane surfaces. However, these surface modification strategies require (i) multistep procedures for surface modification,

(ii) involve the leaching of blended hydrophilic materials from the membrane surface after long-term use, and (iii) are expensive [30-32].

1.3. Antifouling Materials for Surface Modification

Antifouling materials are classified into two major classes namely: polyhydrophilic, and polyzwitterionic materials. The non-fouling polyhydrophilic materials are further classified into (i) polyethylene glycol (PEG), (ii) polysaccharides and (iii) polyamides and the polyzwitterionic materials are further classified into: (i) polybetaines such as 2-methacryloyloxyethyl phosphorylcholine (MPC), sulfobetainemethacrylate (SBMA), and carboxybetaine methacrylate (CBMA) that carry both positive and negative charges on the same monomer, and (ii) polyampholytes such as $-N^+(CH_3)_3$ and $-SO_3^-/-COO^-$, natural amino acids (Glu-, Asp-, Lys+, and Arg+). The antifouling ability of both polyhydrophilic and polyzwitterionic materials is due to the hydration layer formed near the surface of the filtration membranes that acts as a water barrier and prevents the adsorption of foulants on the surface. The mechanism of the formation of a water barrier happens occurs either by (i) hydrogen bonding between the hydrophilic polymeric chains and the surrounding water molecules, or by (ii) ionic solvation between the zwitterionic polymeric chains that contain both positive and negative charges [33]. The schematic representation of chain hydration for hydrophilic and zwitterionic polymers is shown in **Figure 1.3**.

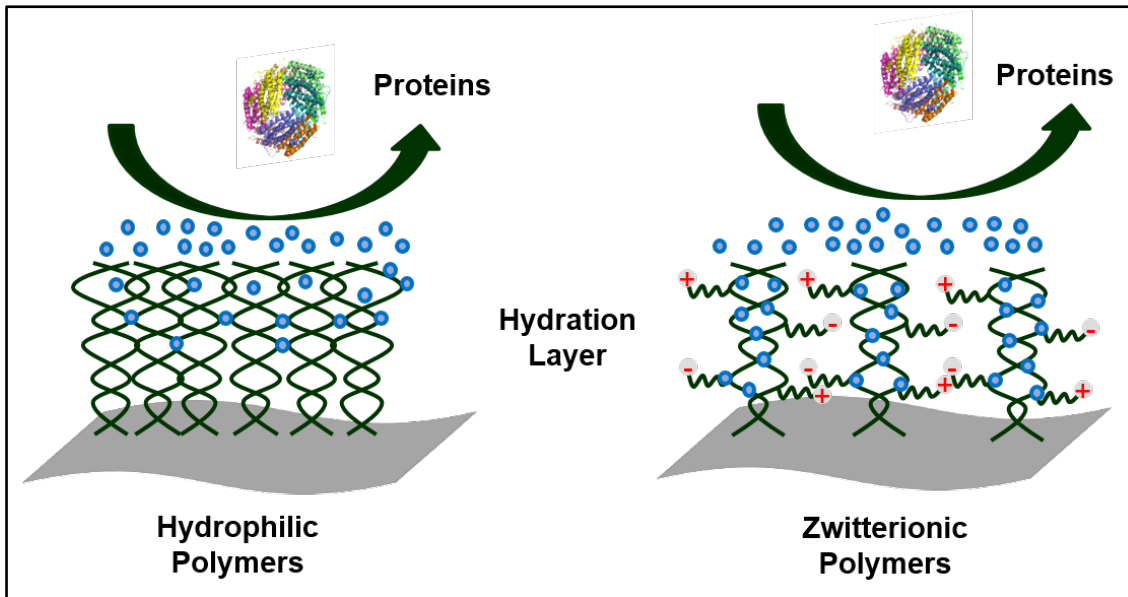


Figure 1.3. Chain hydration mechanism for hydrophilic and zwitterionic polymers.

Figure adapted from [34].

For the past many years, numerous studies have highlighted the potential of both hydrophilic and zwitterionic polymers as excellent antifouling materials. Both hydrophilic PEG-based polymers and polymers containing oligosaccharide moieties are intrinsically anti-biofouling and have demonstrated their anti-fouling ability not only to prevent nonspecific protein adsorption but also towards cell and bacterial adhesion. In the case of zwitterionic materials, their non-fouling ability is determined based on the uniformity of charge distribution and charge neutrality as they have both positive and negative charges on their surface [34].

There are two approaches to modify the surface of the filtration membranes with hydrophilic or zwitterionic polymers to enhance both their hydrophilicity and antifouling properties. The first approach involves the design and direct coating of hydrophilic/zwitterionic polymers on the membrane surface and the second approach involves the design and direct grafting of the polymeric chains on the membrane surface. The schematic representation of coating and grafting of polymeric chains on the membrane surface is shown in **Figure 1.4**.

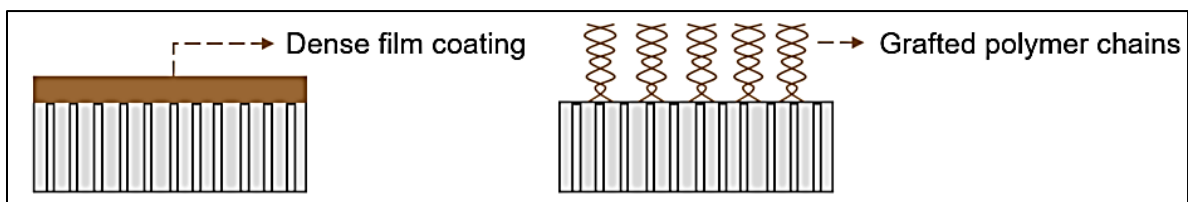


Figure 1.4. Surface modification of filtration membranes via direct coating and grafting of polymeric chains. Figure adapted from [35].

In another approach, the hydrophilic/zwitterionic polymers were grafted onto the surface of the membrane via polydopamine (PDA). It was observed that the hydrophilicity and the antifouling properties of the PDA coated membranes increased significantly and PDA also served as an immobilization platform to covalently anchor a second polymeric layer to further enhance the hydrophilicity and antifouling properties [35].

1.3.1. Mussel-Inspired Surface Chemistry for Surface Modification

Messersmith and co-workers (2007) had reported the development of a simple dip-coating technique of objects for the formation of multifunctional polymer coatings in an aqueous solution of polydopamine. Mussels are promiscuous fouling organisms that attach to both organic and inorganic surfaces and the adhesive proteins secreted by mussels was an inspiration to develop the simple dip-coating technique. Dopamine, a compound containing both catechol and lysine groups was identified to achieve the surface modification of both organic and inorganic substrates. Their hypothesis behind using dopamine for surface modification was by using only catechol containing (DOPA) they could only achieve the surface modification of both inorganic substrates and the electropolymerization of dopamine onto conducting electrodes but achieving the surface modification of organic substrates was elusive. The mussel-inspired surface chemistry-based surface modification approach was achieved by the simple immersion of substrates in an aqueous solution of dopamine in 10Mm tris buffer at a pH of 8.5, similar to the pH of marine environments. This was further followed by the neutralization of dopamine hydrochloride salt results in the spontaneous polymerization of dopamine to give a coating [36].

McCloskey *et al.* (2010) reported the two-step membrane surface modification by depositing polydopamine (PDOPA) and grafting poly(ethylene glycol) (PEG) on polysulfone ultrafiltration (UF) membranes, a poly(vinylidene fluoride) microfiltration membrane and a polyamide reverse osmosis (RO) membrane. The results demonstrated a 96% decrease in BSA adhesion on the membrane surface when modified with PDOPA at a neutral pH. The smallest decrease in water flux measurements of <1% was observed in the case of microfiltration membranes, and the largest decrease of 40% was observed in the case of ultrafiltration membranes. This decrease was attributed towards the reduction in pore sizes of the membranes after their surface modification [37]. In another study, McCloskey *et al.* (2012) had reported the surface deposition of polydopamine (PD) on polypropylene microfiltration (MF), poly(tetrafluoroethylene) MF, poly(vinylidene fluoride) MF, poly(arylene ether sulfone) ultrafiltration (UF), polysulfone UF, polyamide (PA) nanofiltration, and PA reverse osmosis membranes. Further modification of these membranes was performed by grafting poly(ethylene glycol) on the PD modified membranes. The results demonstrated an enhancement in the oil/water fouling resistance in the case of both polydopamine modified membranes and the membranes functionalized with poly(ethylene glycol) [38].

Over the years, a lot of progress has been made in mussel-inspired dopamine chemistry based surface modification approach on filtration membranes to enhance their antifouling properties. However, the limitation involved with this surface modification approach is the requirement for oxidative conditions to obtain the coating [39].

1.4. Prebiotic-Chemistry Inspired Surface Modification

Approach

Prebiotic chemistry is the study of key reactions and molecules that led to the origin of life on earth. Stanley L. Miller (1953) came up with a famous spark experiment using methane, hydrogen and ammonia that produced complex organic compounds such as amino acids thereby initiating the era of experimental prebiotic chemistry. The idea behind this experiment was based on the hypothesis that organic compounds such as methane, ammonia, water, and hydrogen that were present in the earth's atmosphere served as the basis for life.

In this experiment, methane (CH_4), ammonia (NH_3), water (H_2O), and hydrogen (H_2) were circulated in an apparatus past an electric discharge. The electric discharge led to the formation of free radicals and the resulting mixture formed was tested for amino acids using paper chromatography. The experiment was thus concluded by saying that an electrical discharge played a significant role in the formation of primitive compounds in the atmosphere [39]. The apparatus used by Miller in the spark experiment is shown below in **Figure 1.5**.

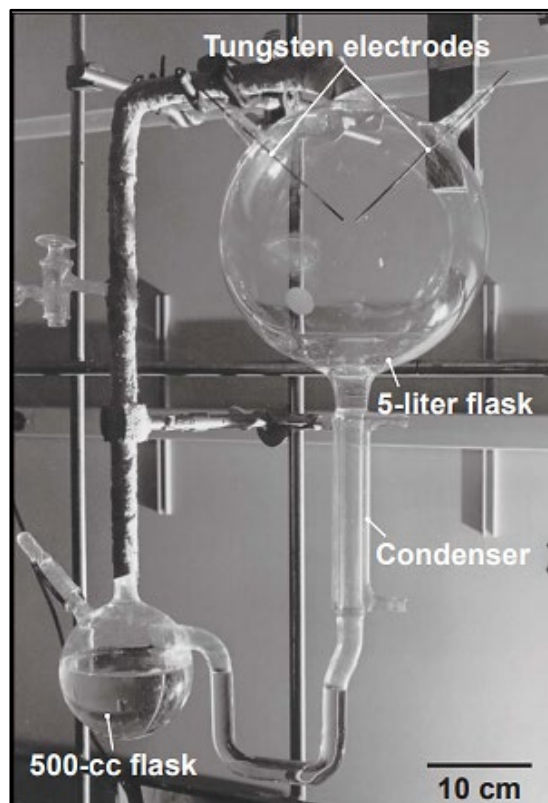


Figure 1.5. The apparatus used for the spark for the experiment. Figure reproduced with permission from [40].

Prebiotic chemistry has always focused on understanding the chemical origin of life and the most studied polymers in the field of prebiotic chemistry are hydrogen cyanide (HCN)-derived polymers as they are a possible source of precursors that provide building blocks for proteins and nucleic acids [38]. Thissen and coworkers proposed a novel and simpler one-step process for coating polymer on various substrates to be used in material science and biomedical applications. They proposed that the can coating process be carried out under (i) oxidative or non-oxidative conditions, (ii) aqueous or non-aqueous solutions and in the (iii) gaseous phase.

The structure of the hydrogen cyanide trimer Aminomalonitrile (AMN) is shown below in **figure 1.6**.

AMN has received a lot of attention, due to its role as a highly reactive synthon in the polymerization of hydrogen cyanide and in the heterocyclic organic synthesis [41, 42].

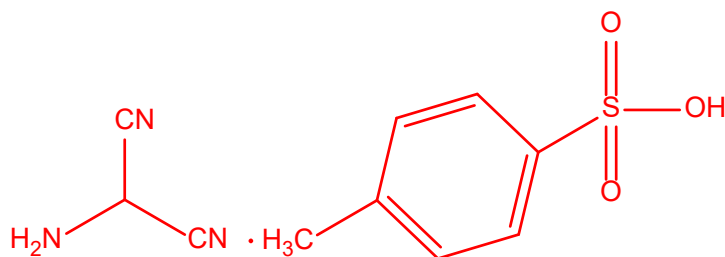


Figure 1.6. Structure of aminomalonitrile (AMN). Figure adapted from [41].

In 2015, Thissen and coworkers had reported the one-step polymerization coating of AMN on a wide range of organic and inorganic substrates. AMN spontaneously polymerizes under buffered aqueous conditions, resulting in a brown nitrogenous polymer complex on the substrate. The cytotoxicity tests were also carried out by seeding the L929 mouse fibroblasts onto the AMN coated tissue culture polystyrene surfaces (TCPS) which resulted in excellent cell attachment and proliferation in areas coated with AMN. These results highlight the potential of AMN to be used in biomedical applications [42]. The simple one-step formation of AMN based coatings is shown below in **Figure 1.7**.

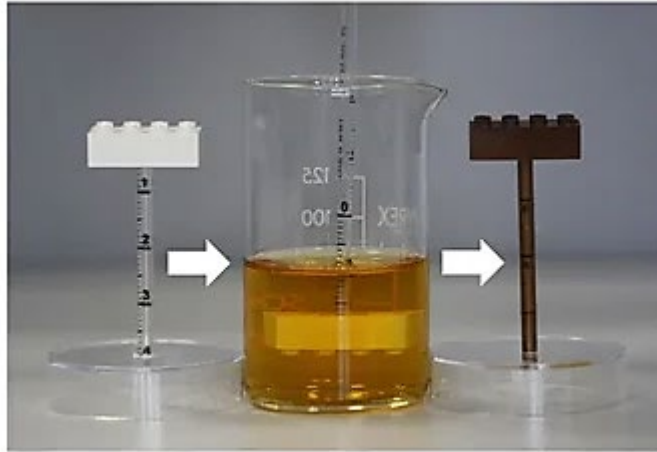


Figure 1.7. The simple one-step procedure of aminomalonitrile (AMN)-based coatings.
Figure reproduced with permission from [42].

The polymers studied in the prebiotic chemistry field offer significant opportunities to be exploited for a wide range of applications ranging from solar cells to implantable medical devices because of their ease in production and a scope for tuning material and chemical properties with the choice of their monomers. The neutralization of the commercially available salt induces the spontaneous polymerization of aminomalonitrile (AMN) in aqueous solutions. Further, this coating chemistry allows for the copolymerization of AMN with a wide range of compounds comprising of one or more functional groups that consisting of amines, hydroxyls, carboxylic acids, carboxylic esters, carboxamides, alkyl halides, etc. and their combinations [41, 42].

1.5. Research Objective

This thesis focusses on the surface modification of a hydrophobic filtration membrane in order to enhance its hydrophilicity and antifouling properties. Numerous studies have reported that surface grafting with hydrophilic/zwitterionic polymers, and/or incorporating inorganic nanoparticles enhance the antifouling and antibacterial properties of the filtration membranes. Therefore, our research goal is to synthesize both hydrophilic and zwitterionic polymers and modify the surface of a commercially obtained PES hydrophobic membrane using the prebiotic-chemistry inspired surface modification approach to enhance its antifouling and antibacterial properties for water purification purposes. The main aim of this research includes:

- i. Synthesis of a hydrophilic glycopolymer (poly(2- lactobionamidoethyl methacrylamide) P(LAEMA) and a zwitterionic polymer (poly(sulfobetaine methacrylate)) P(SBMA).
- ii. Modify the surface of PES membrane first using AMN, followed by the sequential deposition of two different polymers; hydrophilic P(LAEMA) and zwitterionic P(SBMA) on the AMN coated membranes to enhance the antifouling ability of the membrane.
- iii. Incorporate silver nanoparticles (AgNPs) to further enhance the antibacterial properties of the membrane.

CHAPTER 2: POLYMERIZATION AND CHARACTERIZATION TECHNIQUES

2.1. Polymerization Techniques

2.1.1. Living or Controlled Radical Polymerization (CRP)

The CRP technique discovered by Michael Szwarc provides control over the polymer architecture such as thereby resulting in the generation of well-defined polymers with controlled molecular weight, molecular weight distribution, functionality and composition. The CRP technique was developed as there are a few problems that exist with the conventional radical polymerization technique such as poor control over the polymer architecture.

The termination procedure in the CRP technique proceeds until all the monomer is consumed or the polymerization is intentionally terminated thereby minimizing premature termination. The CRP technique is divided into three techniques; Atom Transfer Radical Polymerization (ATRP), Reversible Addition/Fragmentation Chain Transfer Polymerization (RAFT), and Nitroxide-mediated Polymerization (NMP). Among the three techniques the RAFT polymerization technique is more versatile, and does not require any transition metals for polymerization [43-45].

2.1.1.1. Reversible Addition-Fragmentation Chain Transfer (RAFT)

Mechanism

The RAFT process is a living or controlled radical polymerization technique used to synthesize polymers with controlled molecular weights and low polydispersity indices (PDI). This polymerization technique is also used to synthesize block copolymers and polymers with complex architectures that cannot be easily synthesized using the other polymerization techniques. The RAFT technique is very easy to perform and is also compatible with a wide range of functional monomers and reaction media. The steps in the RAFT polymerization technique are: initiation, pre-equilibrium, re-initiation, main-equilibrium, propagation, and termination [46, 47]. The general mechanism of the RAFT polymerization technique is shown in **Scheme 2.1**.

I. Kinetics of RAFT polymerization

1. Initiation

This is the first step in the RAFT polymerization technique and involves the decomposition of the initiator into two radical fragments by reacting with single monomer molecules resulting in the propagation of the polymer chain. The figure below shows the decomposition of the initiator into two radical fragments (I), thereby resulting in the production of a propagating radical (P_1) by its reaction with a single monomer molecule.

2. Propagation

This is the second step in the RAFT polymerization technique, where longer radicals P_{n+1} are formed by the addition of monomer M to the propagating radical chains P_n .

3. RAFT Pre-Equilibrium

This is the third step in the RAFT polymerization technique and is a reversible step because the RAFT adduct radical can lose either the R group (R) or the polymeric species (P_n). In this step, the RAFT agent reacts with the polymeric radical (P_n) to form a RAFT adduct radical thereby resulting in both a polymeric radical and a polymeric RAFT agent ($S=C(Z)S-P_n$).

4. Re-initiation

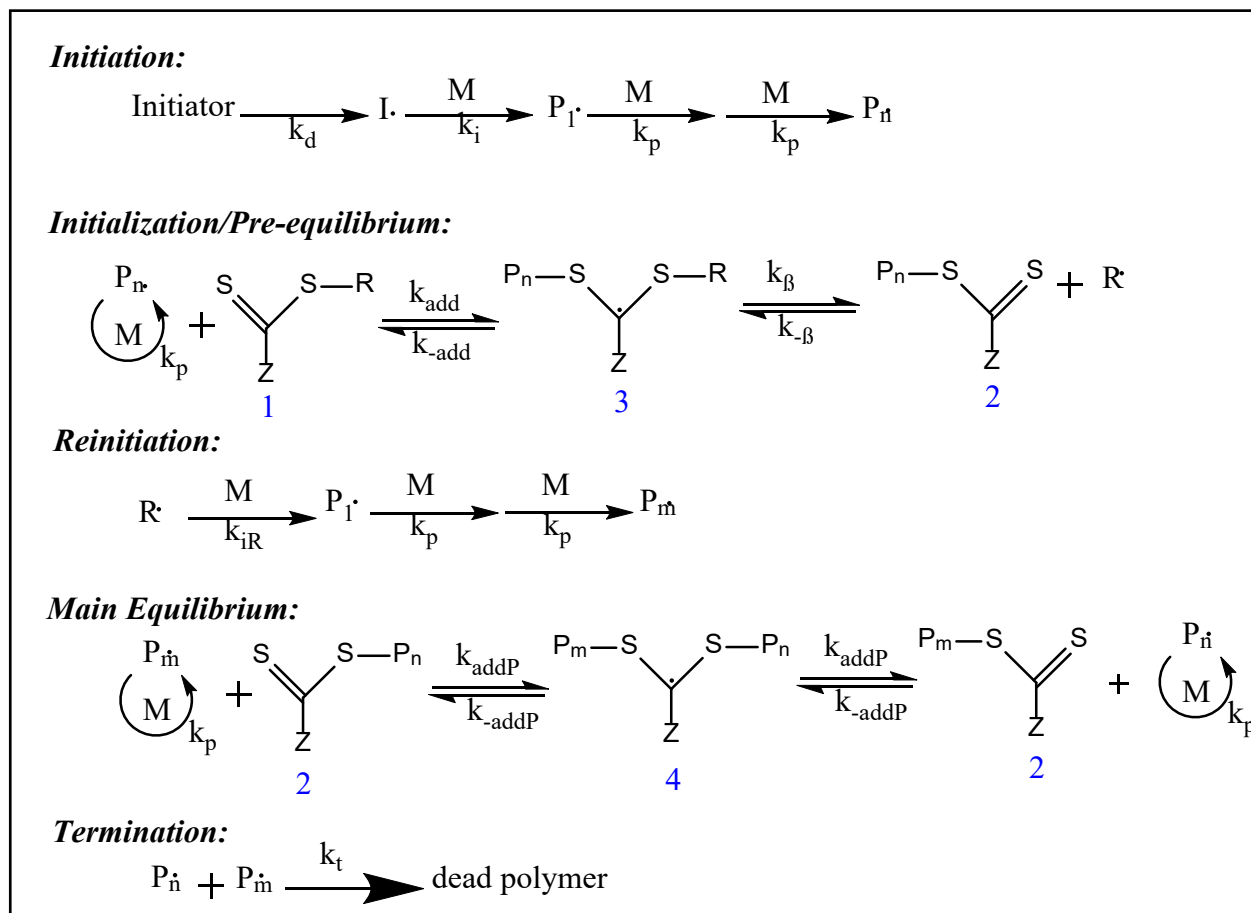
In this fourth step an active polymer chain is formed by the reaction between the (R) group leaving the RAFT adduct and another monomer species.

5. Main RAFT Equilibrium

This is the fifth step of the RAFT polymerization technique and is one of the most important steps because of the rapid interchange occurring between the radicals and the species (P_n and $S=C(Z)S-P_n$) that are not terminated thereby resulting in a polymer chain with a narrow PDI and equal opportunities.

6. Termination

This is the final step involved in the RAFT polymerization technique in which the active polymer chains react to form a dead polymer to form further reactions. This process is called biradical termination and it also obstructs the RAFT adduct radical from preventing the termination reactions.



Scheme 2.1. Kinetics of RAFT polymerization technique. Scheme adapted from [47].

2.2. Characterization Techniques

2.2.1. Nuclear Magnetic Resonance Spectroscopy (NMR)

Nuclear magnetic resonance (NMR) spectroscopy is a powerful analytical technique that was first developed by Bloch and Purcell's research groups in the 1940s. The NMR technique is employed by researchers to elucidate the purity, composition and molecular structures of samples and it also helps in the quantitative determination of the number of molecular groups

in a sample. The analysis is usually performed on condensed phases such as organic, organo-metallic and biological molecules in a solution and on solid-state materials such as glasses and polymers. NMR is unsurpassed in its information content when compared to other analytical techniques and the detailed information about the chemical structure obtained by the NMR determines its versatility. The modern day NMR is run in the Fourier Transform (FT) mode and the other two modes available for generation of NMR signals are swept Continuous Wave (CW) excitation and stochastic excitation [48].

The NMR principle states that the nuclei consists of electrically charged neutrons and protons with inherent spins. Upon the application of an external magnetic field, the nuclear spins align against or with the magnetic field and a transfer of energy occurs from the base energy level to a higher energy level at a wavelength that corresponds to radio frequencies. When the spin returns to its base level, energy is emitted at the same frequency resulting in the generation of an NMR spectra [49]. The isotopes that contain an odd number of protons or neutrons with intrinsic quantum mechanical magnetic moment such as ^1H or ^{13}C are responsible for the NMR structure determination. The nuclear spins of the atomic isotopes are randomly oriented in the absence of an external magnetic field (B_0). However, the nuclear spins are aligned with or against the magnetic field in the presence of an external magnetic field. The molecules that are aligned against the external magnetic field absorb the energy of the magnetic pulse and promote the nuclei to a higher energy state called the A^* state. The molecules that are aligned with the external magnetic field are at a lower energy level called the A state. The energy difference (ΔE) between these two states is related to the magnetic field strength (B_0), and is defined by the equation:

$$\Delta E = h\nu \quad (7)$$

Where, h =Planck's constant and ν =resonant frequency.

The nuclei slowly return to their original equilibrium along the ground state after magnetization (longitudinal and transverse relaxation) of the nuclei by a pulse along the ZXY axis. The chemical shifts of different functional groups within a molecule are determined based on the difference between the longitudinal (T_1) and transverse (T_2) relaxation times. This technique helps in the accurate characterization of the polymers in terms of polymerization, end group analysis, conversion efficiency, molecular weight distribution and stereotacticity [50].

2.2.2. Atomic Force Microscopy (AFM)

Atomic Force Microscopy (AFM) is a type of scanning probe microscopy (SPM) and is the most versatile powerful microscopy technique that is employed to study samples at a nanoscale level. The AFM provides engineers and scientists with both surface measurements and three-dimensional topography of the samples and the images are generated at an atomic resolution along with the height information at an angstrom scale resolution. An AFM has a very sharp probe which interacts with the samples in many different ways to characterize the various properties of the sample such as mechanical property; adhesion, friction and stiffness, electrical property; capacitance, electrostatic forces, electric current, magnetic properties and optical properties. The AFM is a very flexible technique and is a common tool used to characterize materials and achieve nanometer scale resolutions alongside optical and electron microscopy. This technique can also be operated in all kinds of environments such as from ultra-high vacuum to fluids [51, 52]. The schematic representation of the working principle of AFM is shown in **Figure 2.1**.

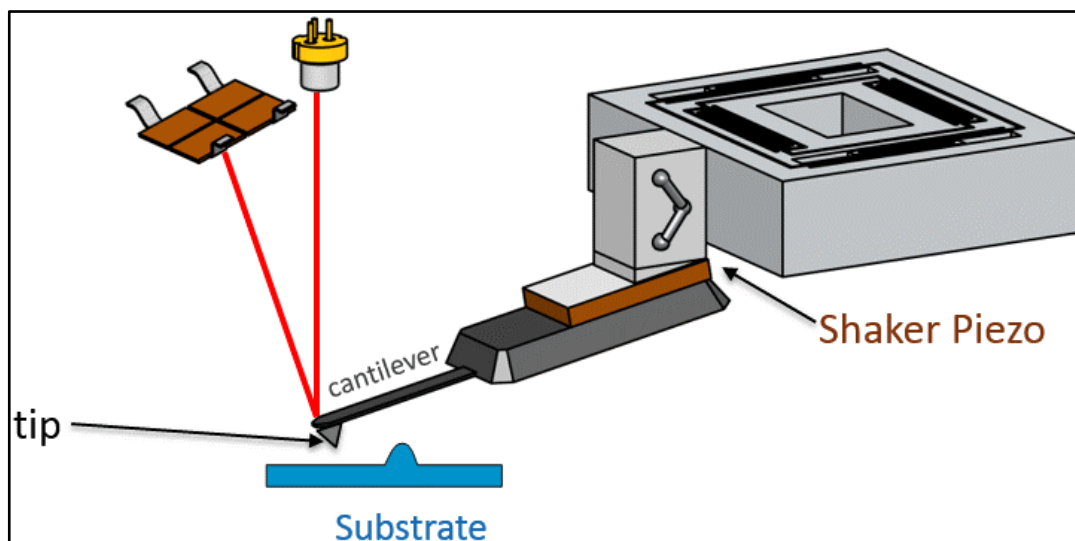


Figure 2.1. Schematics of the working principle of AFM. Figure reproduced with permission from [51].

The AFM consists of a cantilever/tip assembly also referred to as the probe and its principle is based on the cantilever assembly that interacts with the material. The cantilever tip assembly has a very sharp tip with its radius of curvature measuring about 5-10 nm. The

cantilever assemblies are of two types: rectangular and triangular and the height of the cantilever tip varies depending on the type of cantilever. The interaction between the probe and the material that is being characterized occurs through a raster scanning motion. The laser beam reflecting off the cantilever monitors the up or down and side to side motion of the AFM tip as it scans along the surface of the material. A position sensitive photodetector (PSPD) acquires the vertical and lateral motion of the probe and helps in tracking the reflected laser beam.

The AFM cantilever is made up of either silicon or silicon nitride where silicon nitride is mostly used for softer cantilevers with a lower spring constant. The dimensions of the cantilever dictate its stiffness or spring constant and the stiffness of the cantilever governs the interaction of the AFM cantilever tip and the sample surface. The quality of the image obtained is dependent on the chosen AFM cantilever tip and could be poor if the AFM cantilever tip is not carefully chosen. The equation that governs the relationship between the dimensions of the cantilever and spring constant k is given by:

$$k = \frac{Ewt^3}{4L^3} \quad (9)$$

Where, w = width of the cantilever, t = thickness of the cantilever, L = length of the cantilever and E = Youngs' modulus of the cantilever material [51].

2.2.3.1. Modes of Operation

The AFM offers different modes of measurement that enables researchers to characterize the properties of the samples that involve: (1) contact mode, (2) tapping mode and (3) non-contact mode.

I. Contact Mode

In this mode of measurement, the cantilever tip is in close contact with the surface of the sample and the repulsive force on the tip has a mean value of 10^{-9} N. In this mode, the cantilever is pushed against the surface of the sample using a piezoelectric positioning element thereby setting the repulsive force on the tip. The deflection of the cantilever is compared to some desired value of deflection by using a DC feedback amplifier. If there is a difference in the deflection values, a voltage is applied to the piezoelectric positioning element using a feedback

amplifier in order to raise or lower the sample relative to the cantilever such that the desired value of deflection is restored. The voltage applied by the feedback amplifier is the measure of the height of features on the surface of the sample.

The disadvantage of this mode of operation is the application of excessive tracking forces onto the material being characterized by the probe that could result in damaging the material. The effect of tracking force on the material can be reduced by minimizing the application of tracking force on the material [53].

II. Tapping Mode

This mode of measurement generates high resolution topographic images of the samples that are easily prone to damage, are loosely attached to the substrate, or are difficult to image by other AFM techniques. This mode of operation avoids dragging the tip across the surface of the sample by lifting the tip off the surface. This mode also overcomes other problems associated with friction, adhesion, electrostatic forces etc. The cantilever assembly oscillates in ambient air at or near the resonant frequency of the cantilever using a piezoelectric crystal. When the tip is not in contact with the surface of the sample, the piezo motion causes the cantilever to oscillate at a very high amplitude thereby letting the tip move towards the sample until it lightly touches or taps the surface of the sample. The frequency at which the tapping mode contacts and lifts off the surface is 50,000 to 500,000 cycles per second. The oscillation of the cantilever is generally reduced due to the loss of energy that occurs when the tip comes in contact with the surface [53].

III. Non-Contact Mode

The non-contact mode was introduced to avoid the sample damage that occurred in situations where the AFM probe came in contact with the sample. In the non-contact mode, the probe is suspended about 50-150 Angstrom above the surface of the sample. The topographic images of the samples in this mode are constructed by scanning the tip above the surface of the sample and attractive Van Der Waals forces between the tip and the sample are detected. However, these attractive forces from the sample are weaker than the forces in the contact mode. Therefore, to detect the small forces between the tip and the sample, a small oscillation must be given to the tip such that the AC detection methods measure the change in amplitude, phase or

frequency of the oscillating cantilever in response to the force gradients from the sample. The measurement of force gradients from Van der Waals forces which extend only a nanometer from the sample surface generate a high resolution of the sample [53].

2.2.3. X-ray Photoelectron Spectroscopy (XPS)

X-ray photoelectron spectroscopy (XPS) is a quantitative surface analytical technique used to determine the elemental compositions and binding states of the elements on a material. This surface analysis technique is used to analyze elements of sizes ranging from 1-10 nm present on the surface of the sample. The solid surface of the material is irradiated by X-rays while the kinetic energy and the electrons that are emitted from the top of the material being analyzed are measured simultaneously thereby resulting in the generation of the XPS spectra. The number of ejected electrons is counted over a range of electron kinetic energies thus resulting in the generation of a photoelectron spectrum. The identification and quantification of all the surface elements except hydrogen are performed by the energies and intensities of the photoelectron peaks.

The principle of operation of XPS is based on Einsteins' photoelectric effect i.e. most of the materials emit electrons when light is shone upon them. The kinetic energy spectrum of the photoelectrons that are ejected from the surface of a material are due to the irradiating X-rays having a constant energy, $h\nu$, in vacuum. The balance between the kinetic energy of photoelectron E_K , and $h\nu$ is given by the equation:

$$h\nu = E_k + E_B + \phi \quad (10)$$

Where, E_B is the binding energy of the electron, E_K is the kinetic energy, ϕ is the work function of the spectrometer, h is the Planck's constant and ν is the frequency of electrons [54, 55].

2.2.4. Scanning Electron Microscopy (SEM)

A scanning electron microscopy (SEM) creates an image of a surface by using a focused beam of high-energy electrons to generate a variety of signals on the surface. The signals are produced by the interaction between the electrons in the beam and the surface of the sample. The generated signals reveal the surface topography and the composition of the sample. A

particular area is chosen on the surface of the sample and a 2-dimensional image is generated that displays spatial variations in these properties. A conventional SEM with a magnification ranging from 20X to approximately 30,000X and a spatial resolution of 50 to 100 nm can be used to scan areas of width ranging from 5 microns to 1 cm. The chemical compositions of the samples at a particular point on the sample surface is determined using Energy-dispersive X-ray spectroscopy (EDX) and the crystalline structure and crystal orientations are determined using Electron backscatter diffraction (ESBD) [56, 57].

Though an electron microscope is similar to a light microscope, the light in an electron microscope is substituted with electrons and the glass lenses are substituted with electromagnetic/static lenses. The SEM consists of the following components: (i) Electron source, (ii) a column for electrons to travel, (iii) an electron detector, (iv) a sample chamber and (iii) a computer to view the images [58, 59]. The schematic representation of a SEM is shown in figure 2.2.

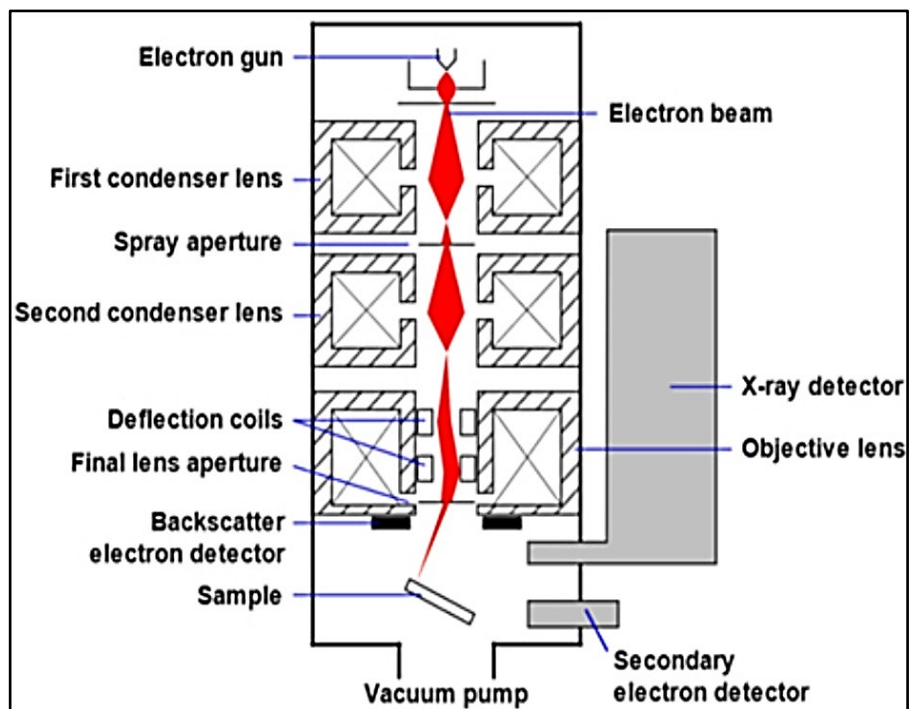


Figure 2.2. The schematic representation of a scanning electron microscope. Figure reproduced with permission from [59].

The sample whose surface morphology needs to be examined is mounted on a stage in a chamber area. The surface of the sample is hit hard by a focused beam of electrons which are produced when the electrons at the top of the column accelerate downwards and pass through a combination of lenses and apertures. The column and the chamber area of the microscope that is designed to operate at low vacuums are evacuated by a combination of pumps. The scan coils situated above the objective lens control the position of the electron beam and allow the electron beams to be scanned over the surface of the sample. These electron beams scanning the surface of the sample provide information about a defined area on the sample to be collected. The electron beams hitting the surface penetrate the sample surface to a few microns. The penetration is based on the factors such as accelerating voltage and the density of the sample. The interaction between the sample and the electrons result in the production of a number of signals that are detected by appropriate detectors. When the electrons come in contact with the samples, they produce secondary electrons, backscattered electrons and characteristic electrons. The signals collected by the detectors result in the formation of images which can then be viewed on the computer screen [58, 59].

2.2.5. Water Contact Angle Measurements

Contact angle (θ) is a traditional quantitative measurement used to determine the hydrophobicity or hydrophilicity of a material by wetting the solid surface of the material using a liquid. Geometrically, an angle is formed at a three-phase boundary where a solid, liquid and gas intersect and the balance between the three is given by the Youngs' equation:

$$\gamma_{SV} = \gamma_{sl} + \gamma_{lv} + \cos\theta_Y \quad (11)$$

Where, γ_{SV} , γ_{sl} and γ_{lv} are interfacial tensions and θ_Y is the Young contact angle.

When the liquid is spread on the surface of the material, its contact angle value is low and if the liquid does not spread on the surface of the material, the contact angle value is high. If $\theta > 90^\circ$, the liquid does not wet the surface, representing non-wetting, whereas if the $\theta < 90^\circ$, the liquid wets the surface, representing complete wetting [60]. The schematic representation of the WCA on a solid surface is shown below in **Figure 2.3**.

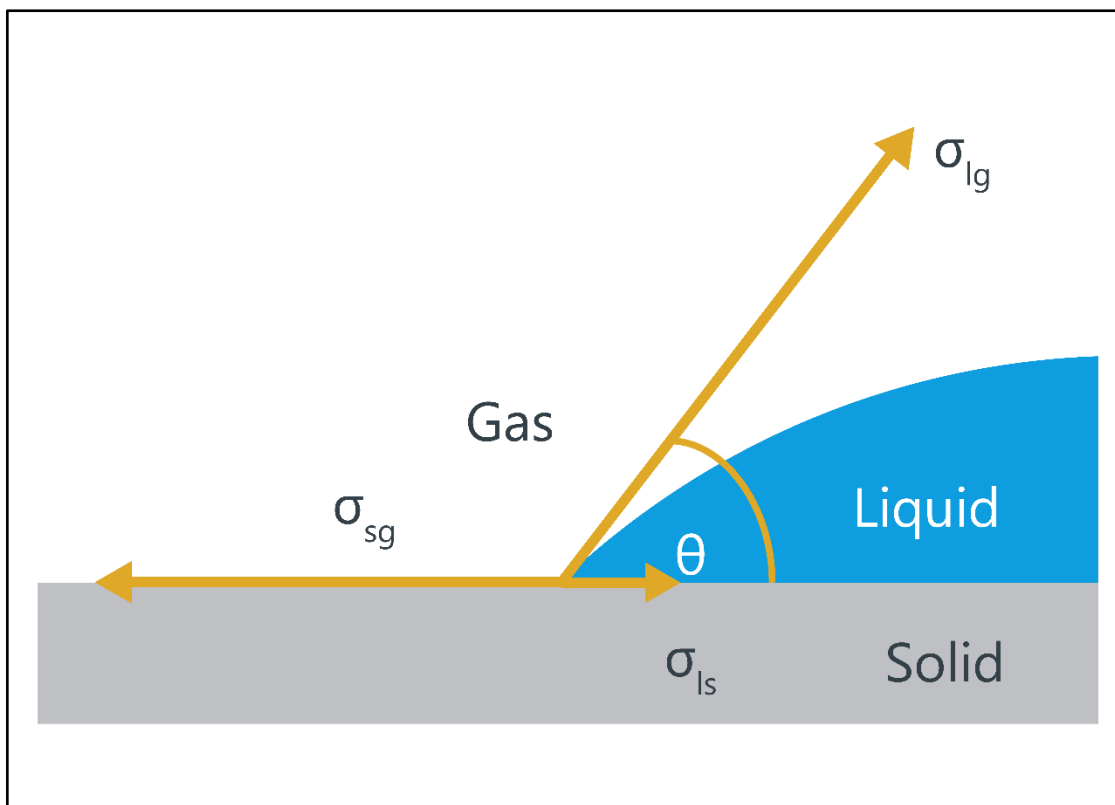


Figure 2.3. Water contact angle measurement on a solid surface. Figure reproduced with permission from [61].

2.2.6. Ultraviolet–Visible (UV-Vis) Spectroscopy

UV-Vis Spectroscopy is a technique used for the quantitative determination of organic and inorganic compounds in a solution. The absorption of visible or ultraviolet light by a chemical compound results in the production of a spectrum. The absorption of ultraviolet radiations by a compound result in the excitation of electrons from ground state to a higher energy state. The chemical structure of the molecule is responsible for the amount of absorption at any wavelength.

The UV-Vis spectrophotometer is based on the Beer-Lambert law which states that the thickness of the absorbing solution containing an absorbing substance that can absorb a beam of monochromatic light which is passed through that solution is proportional to the concentration and incident radiation of that solution. According to the Beer-Lambert law, the absorption of light by the molecules is greater if the molecules capable of absorbing light are greater in number [62]. The equation used to express the Beer-Lambert Law is as follows:

$$A = \log\left(\frac{I_0}{I}\right) = ECI \quad (12)$$

Where, A stands for absorbance, I_0 refers to intensity of light on the sample cell, I refers to the intensity of light departing the sample cell, C refers to the concentration of the solute, L refers to the length of the sample cell and E refers to the molar absorptivity.

CHAPTER 3: PREBIOTIC-CHEMISTRY INSPIRED POLYMERIC COATINGS OF POLYETHERSULFONE (PES) ULTRAFILTRATION MEMBRANES FOR ENHANCED ANTIFOULING AND ANTIBACTERIAL PROPERTIES

3.1. Introduction

The inadequate supply of clean water is one of the greatest challenges that has greatly affected the sustainable development of industrial and societal activities. Though several water-purification technologies have been developed, their drawbacks include high energy consumption, operational costs and production of harmful chemical by-products. This has led to the emergence of membrane technology, an attractive and environmental-friendly water-purification approach. Membrane technology involves the use of water purification membranes such as microfiltration (MF), nanofiltration (NF), ultrafiltration (UF) and reverse osmosis (RO) membranes that can remove contaminants ranging from bacteria in microns to ions in angstroms [63-65]. Both ceramics and polymers are employed in the preparation of water purification membranes. However, due to the brittle nature and high production costs of ceramic membranes, polymeric membranes are more commonly used in membrane technology for water-treatment. The most commonly employed polymer for the preparation of water-purification membranes is Polyethersulfone (PES).

PES is a polymer consisting of repeating ether units and sulfone linkages alternating between aromatic rings. It has a high glass transition (T_g) temperature and excellent mechanical, thermal and chemical properties due to which the PES polymer has been widely employed in the preparation of water-purification membranes such as microfiltration, ultrafiltration and nanofiltration membranes for a wide-variety of applications [66, 67]. The chemical structure of PES is shown in **Figure 3.1**. However, the employment of PES membrane for water purification is restricted due to its intrinsic hydrophobicity which results in the adsorption of proteins or bacteria onto the surface of the membrane thereby

resulting in membrane fouling. Fouling in membranes occurs due to the physicochemical interactions between the membrane surface and the foulants in feed water and this further reduces the water flux of the filtration membranes either permanently or temporarily [63, 64, 66, 68, 69].

An effective technology to prevent or reduce membrane fouling is the hydrophilic surface modification of the membrane surface. Enhancing the hydrophilicity of the membrane surface, results in the creation of a buffer layer with water molecules on the membrane surface thus enhancing the anti-fouling properties of the membrane [70]. Many surface modification techniques have been implemented in the past, to enhance the surface hydrophilicity of the membranes [68]. However, the above mentioned surface modification approaches have their own limitations such as (i) desorption of adsorbed coatings under chemical conditions, (ii) multi-step procedures for implementation of coatings and (iii) use of complex instrumentation. A summary of previously used surface modification approaches is shown in **Table 3.1**.

Base material	Modification method	Findings	References
PES ^a	Adsorption	Increase in the rejections of BSA, PEG, dextran, and surfactant solutions	Hvid et al. [71]
PS ^b	N ₂ plasma treatment	Low protein fouling and high flux recovery	Gancarz et al. [72]
PAN ^c	sodium hydroxide treatment	Increased antifouling and hydrophilicity	Qiao et al. [73]
PP ^d	N ₂ plasma-induced grafting of sugar containing monomer	Increase in flux and fouling resistance	Kou, Rui-Qiang, et al. [74]
CA ^e	Grafting of PEG by using sodium persulfate as an oxidizing agent	An increase in water flux by 15-25% compared to pristine membranes	Gullinkala et al. [75]

Table 3.1. A summary of the previous surface modification strategies;

^aPolyethersulfone, ^bPolysulfone, ^cPolyacrylonitrile, ^dPolypropylene, ^eCellulose Acetate

Hence, Messersmith and co-workers (2007) reported the development of a simple dip-coating technique of objects for the formation of multifunctional polymer coatings in an aqueous solution of polydopamine. In this surface modification approach, the neutralization of dopamine hydrochloride salt results in the spontaneous polymerization of dopamine to give a coating. For example, Tang et al. (2015) had reported the modification of polysulfone membranes with polydopamine (PDA) and silver nanoparticles for the mitigation of biofouling and Haider et al (2016) had reported the immobilization of silver nanoparticles on the surface of aminated polyethersulfone for controlled silver ion release for antibacterial and water treatment applications [77, 78]. However, the limitation involved with this process is the requirement for oxidative conditions to obtain the coating [76]. Therefore, in our study we report a robust and facile dip-coating technique for the surface modification of the hydrophobic PES membrane using the prebiotic-chemistry inspired approach to enhance the hydrophilicity, antifouling and antibacterial properties of the membrane surface.

Prebiotic chemistry is the study of key reactions and molecules that led to the origin of life on earth. The most studied polymers in the field of prebiotic chemistry are hydrogen cyanide (HCN)-derived polymers as they are a possible source of precursors that provide building blocks for proteins and nucleic acids. Thissen and coworkers (2013) proposed a novel and facile one-step polymeric surface modification approach on various substrates for material science and biomedical applications. They had proposed that the coating process be carried out under (i) oxidative or non-oxidative conditions, (ii) aqueous or non-aqueous solutions and in the (iii) gaseous phase. Aminomalonitrile (AMN), a trimer of hydrogen cyanide has received a lot of attention, due to its role as a highly reactive synthon in the polymerization of hydrogen cyanide and in the heterocyclic organic synthesis [79-81]. The structure of the hydrogen cyanide trimer Aminomalonitrile (AMN) is shown in **Figure 3.1**.

Thissen *et al.* (2015) had reported the one-step polymerization coating of AMN on a wide range of organic and inorganic substrates. AMN spontaneously polymerizes under buffered aqueous conditions, resulting in a brown nitrogenous polymer complex on the substrate. In this study, the cytotoxicity tests were also carried out by seeding the L929 mouse fibroblasts onto the AMN coated tissue culture polystyrene surfaces (TCPS) which resulted in excellent cell attachment and proliferation in areas coated with AMN. These results highlight the potential of

AMN to be used in biomedical applications [80]. Menzies *et al.* (2017) had reported the prebiotic chemistry inspired coating of silicon substrates with a goal to produce new and improved bone-contacting medical devices with excellent bioactivity at the interface. The coatings were presented with and without the incorporation of comonomers 3,4-di- and 3,4,5-trihydroxy benzaldehyde (DHBA and THBA). The results demonstrated that the incorporation of HBA monomers improved the polymerization kinetics, surface morphology and chemistry compared to the AMN only coatings. Further, the cytotoxicity tests performed showed an increase in cell proliferation on the AMN/HBA coatings [81].

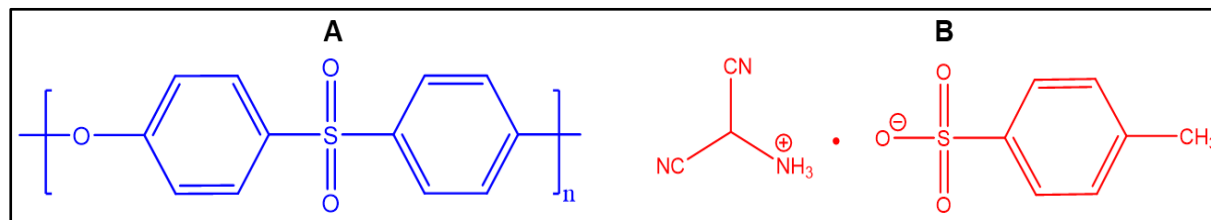


Figure 3.1. Chemical structures of polyethersulfone (A) and aminomalonitrile p-toluenesulfonate (B). Figure (B) adapted from [81].

A lot of research has been carried out to covalently anchor hydrophilic and zwitterionic polymers onto the filtration membranes that have been pre-modified with PDA. Both hydrophilic and zwitterionic polymers form a hydration layer near the surface of the filtration membrane to prevent the adsorption of foulants on the surface. Thus, based on the previous studies we report a simple and novel prebiotic-chemistry approach to achieve polymeric coatings which involves the spontaneous polymerization of aminomalonitrile (AMN). The hydrogen cyanide monomeric units (HCMUs) consist of at least one nitrile functional group and one nucleophilic functional group such as amine (NH) or thiol (SH) that undergo self-polymerization. The self-polymerization of AMN is induced by neutralizing the commercially available salt in simple aqueous solutions. The HCMUs can also be copolymerized with ligands containing one or more functional groups, but these comonomers should comprise of functional groups that react with amines, nitrile or any intermediate formed during the polymerization of HCN [79].

Therefore, it is hypothesized that the pre-modification of the PES membrane surface with AMN, followed by the grafting of the hydrophilic glycopolymer, P(LAEMA) and a zwitterionic

polymer, P(SBMA) will result in the enhancement of both surface hydrophilicity and the antifouling properties of the hydrophobic PES membrane. Further, the deposition of silver nanoparticles on the modified membrane surfaces will further improve the antibacterial properties of the PES membrane. The schematic representation of the hypothesis is shown in **Figure 3.2**.

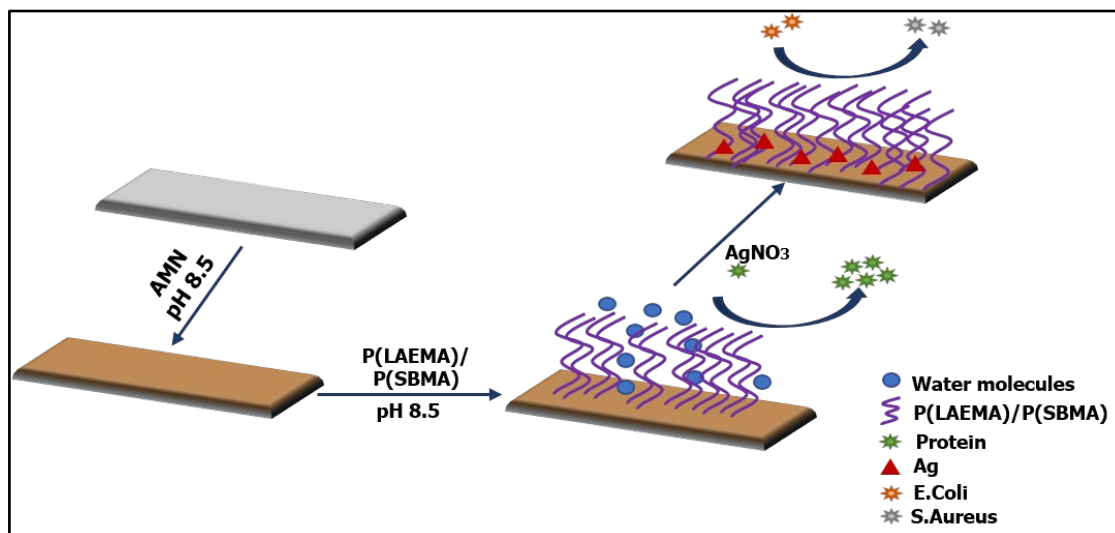


Figure 3.2. Schematic representation of the prebiotic-chemistry inspired polymeric coating.

3.2. Experimental

3.2.1. Materials

Polyethersulfone ultrafiltration membranes with a molecular weight cut-off (MWCO) of 100kDa was provided by Sterlitech Corporation (Kent, WA). Aminomalononitrile *p*-toluenesulfonate, azobis(4-cyanovaleric acid) (ACVA), silver nitrate (AgNO₃), and bovine serum albumin (BSA) were purchased from Sigma-Aldrich and used without further purification. LIVE/DEAD BacLight Bacterial Viability Kit L-7012 were purchased from Thermo Fisher Scientific Inc. *Escherichia coli* (*E. coli*) (ATCC 25922) and *Staphylococcus aureus* (*S. aureus*) (ATCC 25923) (ATCC, USA) were used as model bacteria in all bacterial tests. Luria-Bertani broth (LB) and tryptic soy broth (TS) (Fisher Scientific, USA) were used as liquid media for *E. coli* and *S. aureus*, respectively.

3.2.2. Methods

3.2.2.1. Polymer Synthesis and Characterization

The monomer LAEMA and the chain transfer agent (CTA) cyanopentanoic acid dithiobenzoate (CTP) were synthesized in the laboratory according to reported protocols [20, 21]. The homopolymers P(LAEMA) and P(SBMA) were synthesized using the RAFT polymerization technique in the presence of the initiator 4,4'-azobis(4-cyanovaleric acid) (ACVA) and the chain transfer agent (CTA) used in the case of RAFT is 4-cyanopentanoic acid dithiobenzoate (CTP). The structures of ACVA and CTP are shown in **Figure 3.3**.

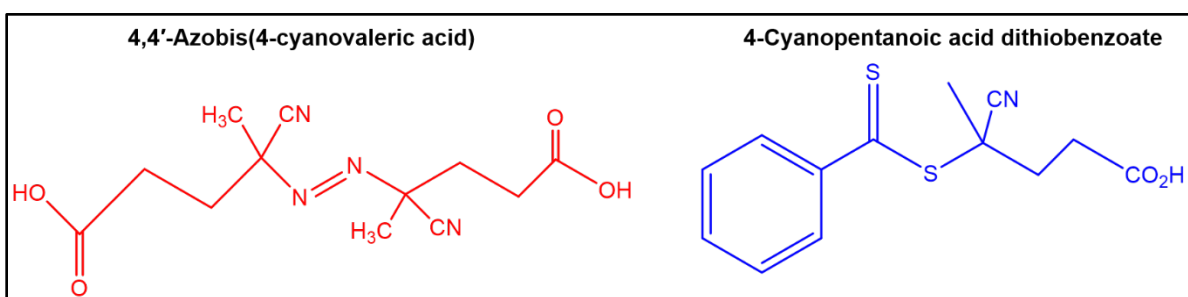


Figure 3.3. Chemical structures of ACVA and CTP.

Briefly, for the synthesis of P(LAEMA), the monomer LAEMA, ACVA and the chain transfer agent CTP were dissolved in *N,N'*-dimethylformamide (DMF) inside a 50 mL polymerization tube. The mixture was then degassed with nitrogen for 30 mins and the reaction was carried out by maintaining the temperature of the oil bath at 70 °C for 24 h under constant stirring. The reaction was terminated by quenching with liquid nitrogen and exposure to air. The obtained polymer was then purified by dialyzing it against distilled water (DI) for 3 days followed by lyophilisation to obtain the polymer as a powder. The same procedure was followed for the synthesis of the homopolymer P(SBMA) using the solvent 2,2,2-trifluoroethanol (TFE). The structural composition of the obtained homopolymers was confirmed by ¹H NMR spectroscopy (Varian 500 NMR). The synthesis mechanism of the homopolymers, P(LAEMA) and P(SBMA) using the RAFT polymerization technique is shown below in **Figure 3.4**.

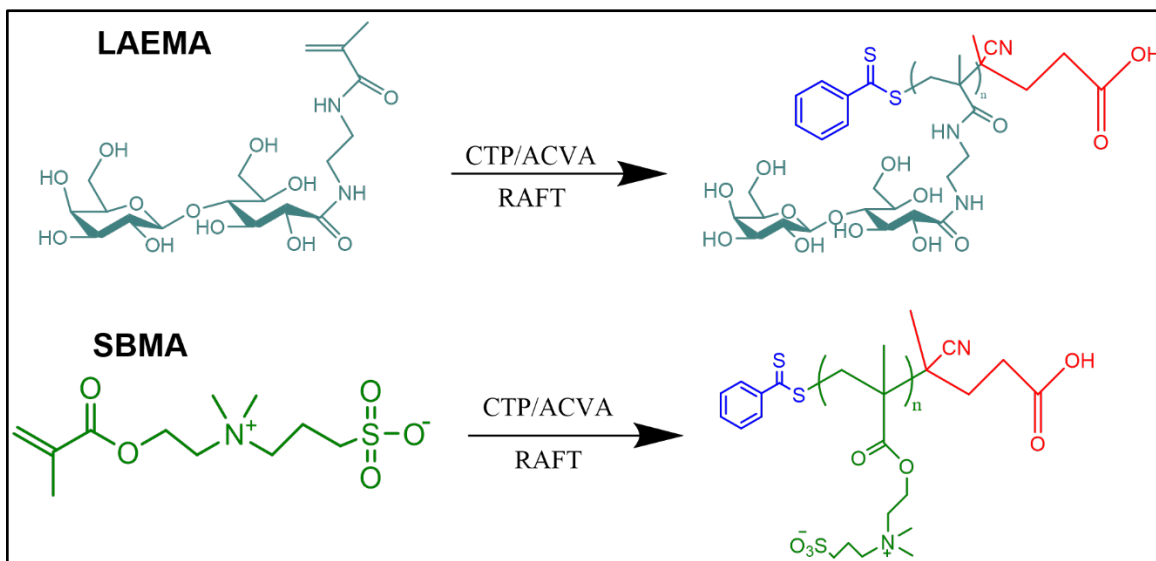


Figure 3.4. The schematic representation of the RAFT polymerization mechanism.

3.2.2.2. Membrane Pre-treatment and Surface Modification

Prior to their usage, the PES membranes samples were first soaked in excessive ethanol for 24 hours. Then the membranes are rinsed and immersed in deionized (DI) water for another 24 hours. The following procedure is carried out to remove the pore blocking agents.

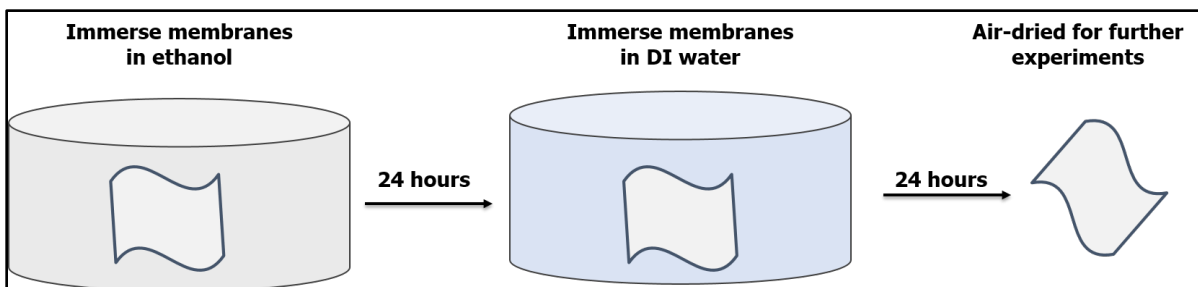


Figure 3.5. Schematic representation of pre-treatment of filtration membranes.

For the preparation of membranes with antibacterial and antifouling properties, the surface modification of the PES UF membranes was performed as follows: (i) the first step involves the preparation of a 1wt/v% stock solution of aminomalonnitrile (AMN) using pure phosphate buffer saline (PBS). The pH of the stock solution was then adjusted to 8.5 using 1M NaOH to initiate the polymerization. The AMN stock solution was then poured into a petri-dish and the membrane was immersed into the stock solution by the active side facing downward. The membrane is left untouched for 24 hours. The presence of adherent coating on the membrane surface was indicated by a light brown color change.

The second step involves the preparation of antifouling membranes, the pH of the prepared P(SBMA) and P(LAEMA) was also adjusted to 8.5 using 1M NaOH. The membranes were again left untouched for 24 hours. The modified membranes were further rinsed with DI water, and then air-dried for further characterizations [80-84]. The schematic representation of the coating process is shown in **Figure 3.6**.

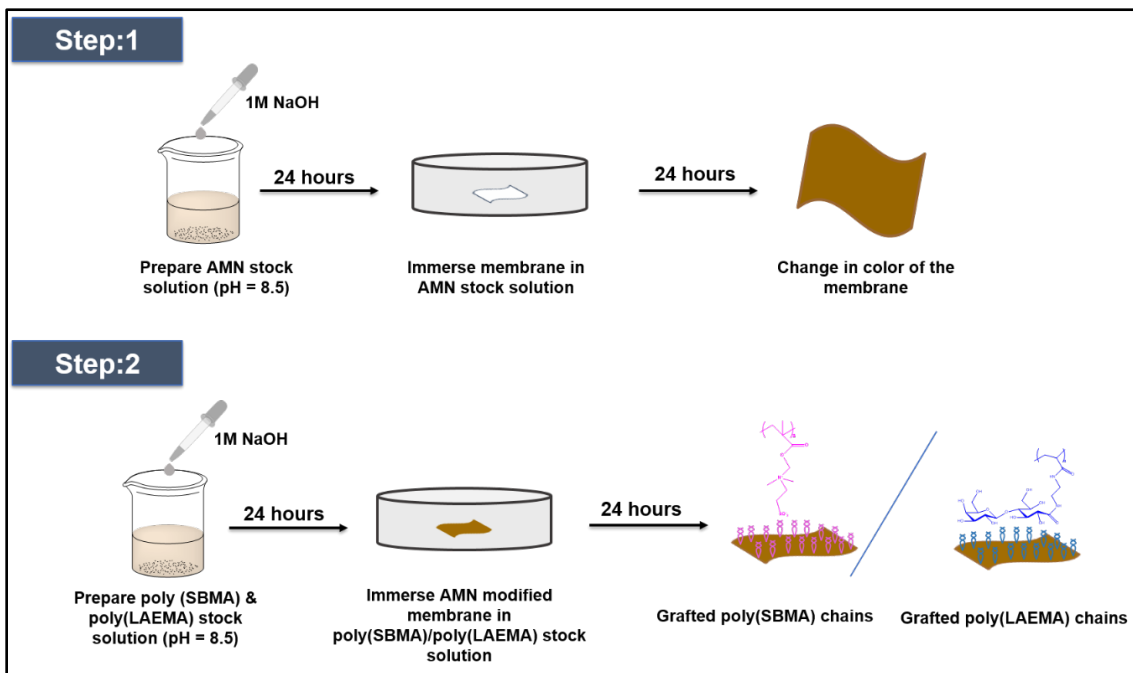


Figure 3.6. Schematic representation of the membrane coating process.

3.2.2.3. Membrane Surface Characterizations

The surface morphology of the membranes and the elemental analysis of the membranes deposited with silver nitrate was observed using the scanning electron microscopy (Tescan Vega-3 SEM with EDX). The X-ray photoelectron spectroscopy (XPS) was performed using an AXIS Nova spectrometer (Kratos AXIS Ultra) and the Fourier-transform infrared spectroscopy (FTIR) was performed using a (Nicole is50 FTIR) spectrometer (Thermo Fisher Scientific) with attenuated total reflection (ATR) mode to evaluate the surface chemical composition of the membranes.

The AFM imaging of the membranes was carried out to determine the surface roughness of the membranes using Dimension Icon AFM (Bruker, Santa Barbara, CA). The surface

wettability of the membranes was determined using the (Ramé-hart instrument co, Succasunna, NJ, USA).

3.2.2.4. Static Protein Adsorption Tests

The antifouling ability of the membranes was evaluated by conducting the static protein adsorption tests. The membranes with an area of 1.0 cm×1.0 cm were immersed in phosphate buffered solution (PBS) BSA for 3 hours at room temperature. The membranes were subsequently washed with PBS to remove the loosely bound protein on the membrane surface and then immersed in 2wt% of sodium dodecyl sulphate. The amount of protein adsorbed on the membrane surface was calculated using the Micro BCA™ Protein Assay Reagent Kit (PIERCE) [85]. The schematic representation of the protein adsorption tests performed on the membrane is shown in **Figure 3.7**.

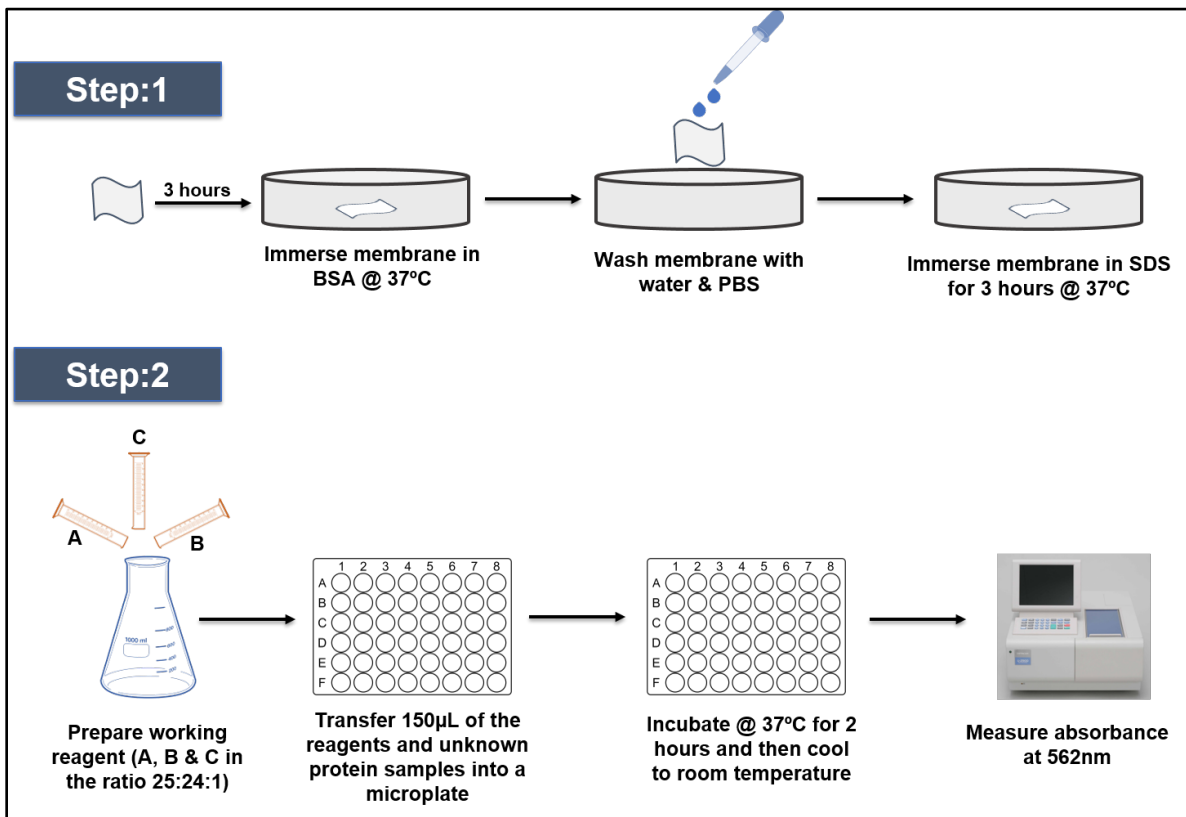


Figure 3.7. Schematic representation of the static protein adsorption steps; (Step 1) membrane preparation for fouling tests, (Step 2) BCA assay protocol for quantifying the protein content.

3.2.2.5. Antibacterial Studies

The bacterial strains *Escherichia coli* (*E. coli*, Gram negative) and *Staphylococcus aureus* (*S. aureus*, Gram positive) were used as the model bacteria to determine the bactericidal activity of the membranes. The inhibition zone method was used to investigate the bactericidal activity of the modified membranes. The membranes were sterilized and placed on *E. coli* and *S. aureus* agar plates at an inoculum concentration of 10^9 cells mL^{-1} bacteria and incubated at 37 °C for 24 hours. The antibacterial activity of the membrane samples was recorded using a digital camera and was confirmed by the halo zone formed around the samples after 24 hours [86, 87].

3.3. Results and Discussion

3.3.1. Polymer Synthesis and Characterization

The homopolymers P(LAEMA) and P(SBMA) were synthesized using the RAFT polymerization technique in the presence of 4,4'-azobis(4-cyanovaleric acid) (ACVA) as the initiator, 4-cyanopentanoic acid dithiobenzoate as the chain transfer agent, and dimethylformamide (DMF), and 2,2,2-Trifluoroethanol as solvents respectively. The obtained polymers were then characterized by ^1H NMR in the presence of deuterium oxide (D_2O) as the solvent. The ^1H NMR spectra of the two polymers is shown in **Figure 3.8**.

From **Figure 3.8 (a)**, the solvent peak can be seen at 4.79 ppm, and the signals of the polymer chains (3, 4) can be seen at (δ 3.61 ppm), and (1, 2, 8, 10, 13) can be seen at (δ 1.09, 1.94, 4.46, 4.24, 4.61 ppm) respectively. As shown in **Figure 3.8 (b)**, the solvent peak can be seen at 4.79 ppm and the peaks of the RAFT aromatic end-group signals (h, I, j) can be seen between (δ 7.58 to 8.06 ppm). The polymer side chain signals (6, 3, 1, 2) can be seen at (δ 3.04, 3.29, 4.56, 3.86 ppm) respectively [88, 89].

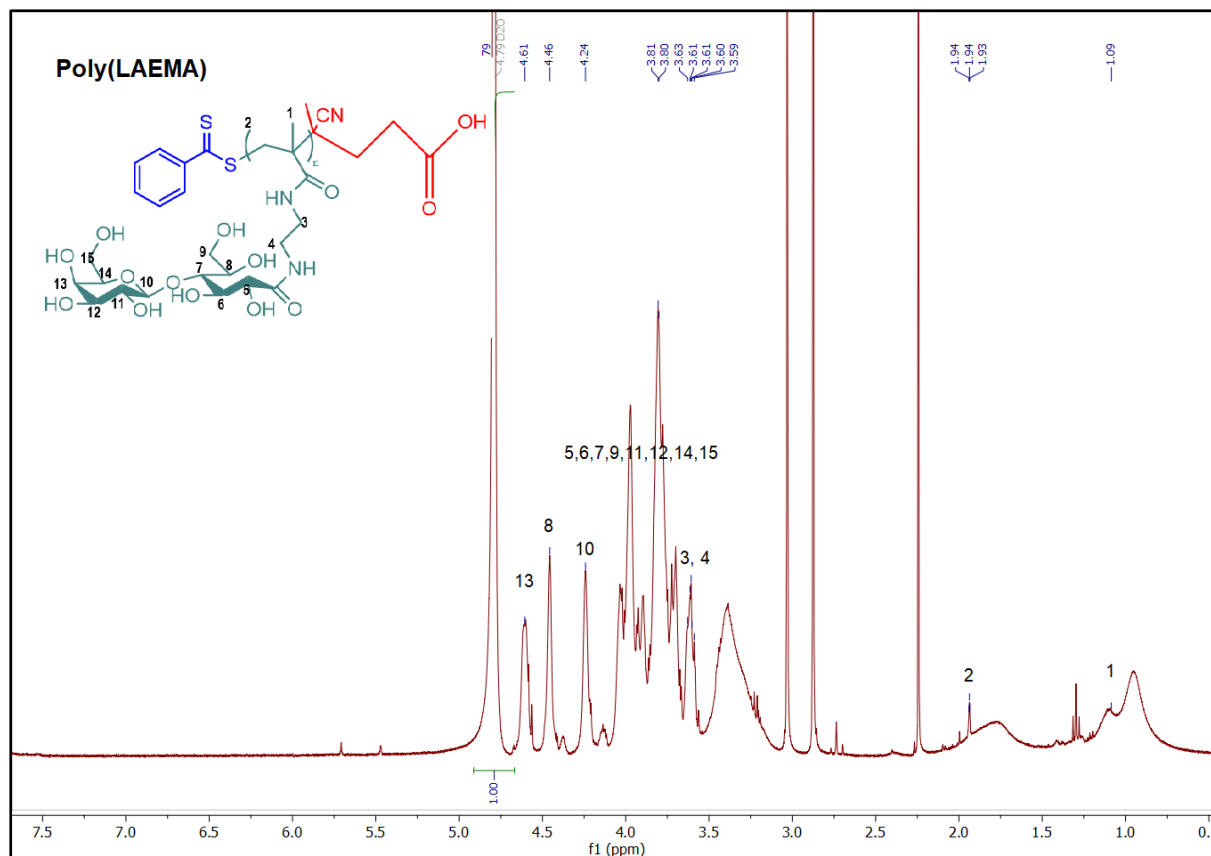


Figure 3.8 (a). ^1H NMR spectra of P(LAEMA) in D_2O .

3.3.2. Surface Chemical Composition of the Membranes

The surface chemical composition of the modified membranes was evaluated using XPS. As shown in **Figure 3.9**, the pristine PES membrane exhibited the C 1s, O 1s and S 2p peaks at binding energies of 282.16 eV, 528.97 eV and 165.03 eV respectively. The successful deposition of AMN was confirmed by the occurrence of a new N 1s peak at a binding energy of 396.8 eV. The reason behind this could be attributed towards the highly nitrogenous character of the AMN coatings [80]. Meanwhile, the intensity of the S 2p peak in the case of the membrane modified with decreased which indicated that the surface of the pristine PES membrane was completely covered by AMN. However, the reoccurrence of the S 2p peak at a binding energy of 165.3 eV on the surface of the AMN/P(SBMA) indicated the successful deposition of P(SBMA) on the membrane surface. The intensity of the S 2p peak at decreased in the case of the membrane modified with AMN/P(LAEMA). Furthermore, the successful deposition of P(LAEMA) was confirmed by the occurrence of the O 1S peak and the C 1s peak at binding energies of 529.4 eV and 281.9 eV respectively.

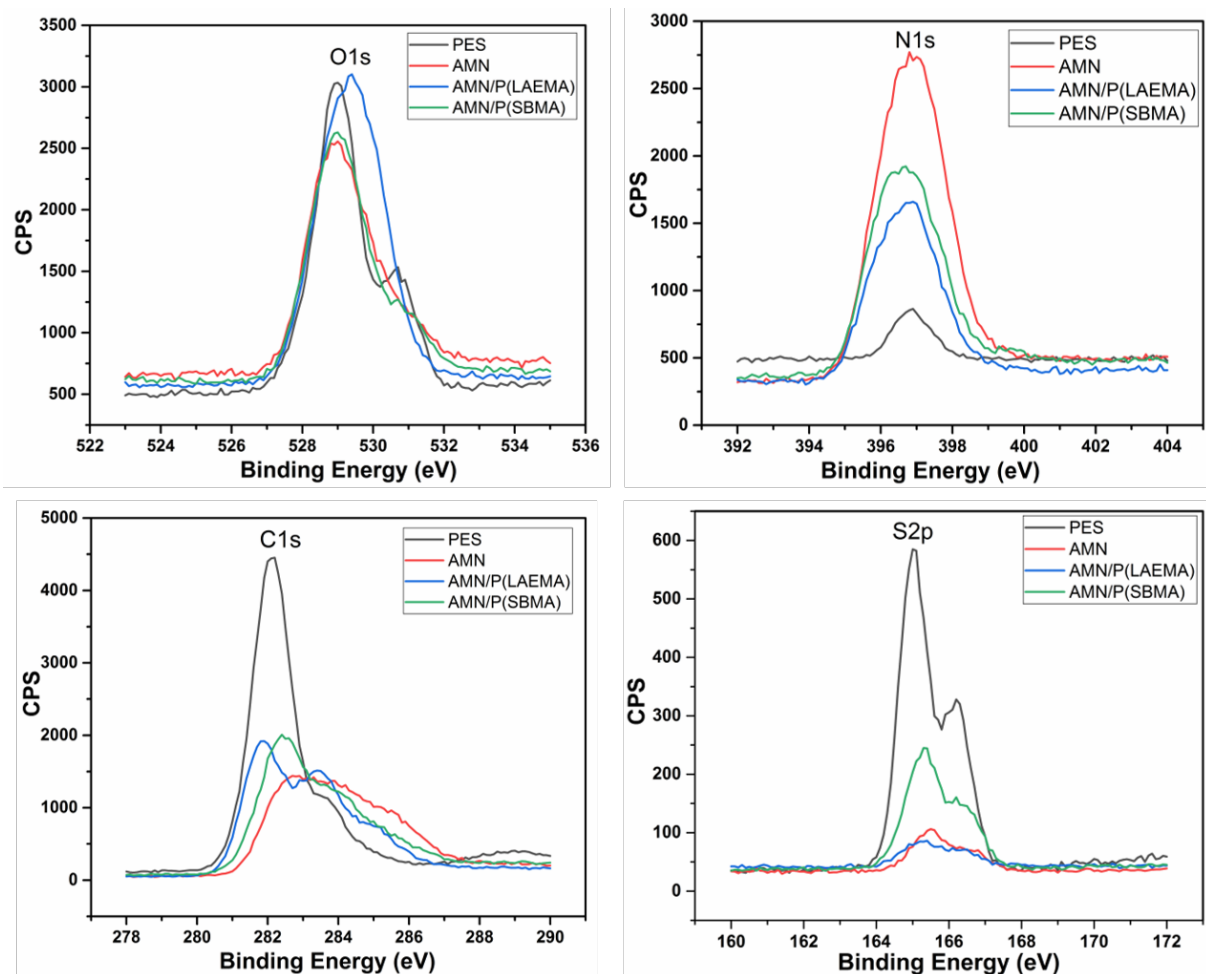


Figure 3.9. XPS spectra of the modified and unmodified membranes.

The surface of the membranes deposited with silver nanoparticles (AgNPs) were analyzed using EDX to determine the Ag elemental contents. The membrane surfaces were modified with 0.1M concentration of silver nitrate solution and the surfaced modified with the highly nitrogenous AMN are believed to complex strongly with various metals ions [79]. Due to the incomplete structural knowledge of the coating, there is no proper indication regarding the mechanism involved in the binding of silver ions or the formation of metallic silver on the AMN coated surfaces. However, two possible mechanisms for the deposition of silver could be due to the disproportionation reactions of silver in the presence of certain functional groups, or the presence of nucleophilic amines and nitriles which donate electrons to form metal coordination complexes [80]. As shown in **Table 3.2**, and in **Figure 3.10**, the silver content on the unmodified PES membrane was low when compared to silver content on modified membranes.

This could be due to the penetration and uniform distribution of silver due to the metal coordination complexes formed on the modified surfaces.

Membranes	C	O	S	Ag
PES/Ag	61.98	30.72	5.26	1.55
AMN/Ag	58.75	38.32	0.71	2.23
AMN/P(LAEMA)/Ag	58.67	35.03	3.70	2.60
AMN/P(SBMA)/Ag	61.65	28.95	6.48	2.92

Table 3.2. Surface elemental composition of AgNPs deposited on the surfaces of modified and unmodified membranes.

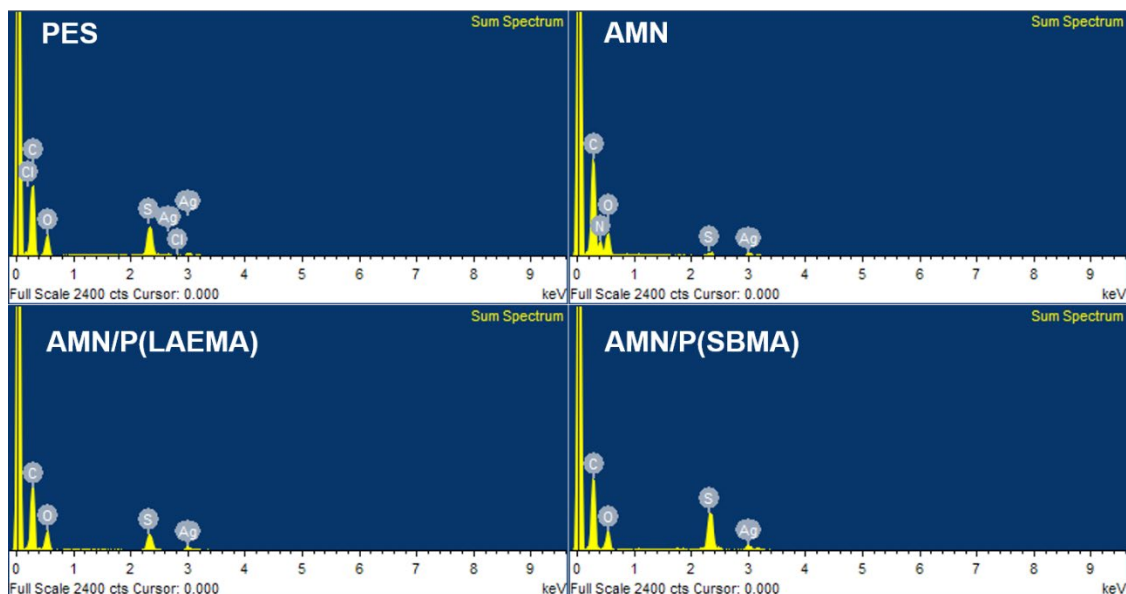


Figure 3.10. EDX images of the modified and unmodified membranes deposited with AgNPs.

3.3.3. Surface Wettability and Roughness of the Membranes

The surface wettability of the membranes is one of the key factors that could affect the surface protein interactions. An increase in surface hydrophilicity results in better fouling resistance. This is because when a hydrophilic surface comes in contact with water, the water molecules form a hydration layer around the membrane surface due to the hydrogen-bond interaction between the hydrophilic surface and the water molecules. The hydrophilic/hydrophobic property of a material can be determined using the static water contact angle (WCA) measurements.

In this study, the WCA measurements for the modified membranes was measured in air. As shown in **Figure 3.11**, the WCA of the pure PES membrane was 77.9°. All the modified surfaces showed lower contact angle measurements which demonstrates an enhancement in their hydrophilicity. Among these, the membrane modified with P(SBMA) demonstrated the lowest WCA of 13.3°, thereby indicating a stronger hydration capacity of this membrane.

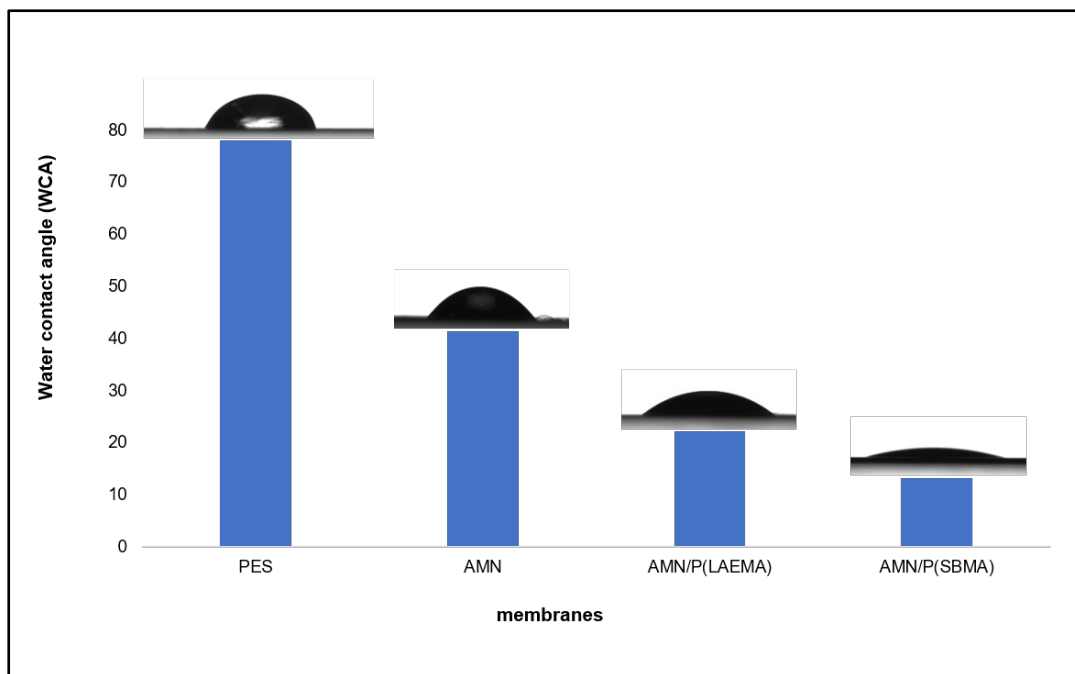


Figure 3.11. Static water contact angle measurements of the modified and unmodified membranes.

The surface roughness of the membrane is another important feature that could affect the antifouling ability of the membranes. As shown in **Figure 3.12**, the surface of the pristine PES membrane was smoother with a root-mean-square (RMS) roughness of 12.3 nm and in the case of the membrane modified with AMN, the RMS roughness increased to 19.9 nm. The reason behind this could be due to the formation of precipitates during the aqueous polymerization of AMN. However, with the introduction of P(LAEMA) and P(SBMA) the surface roughness of both the membranes decreased to 5.99 nm and 4.05 nm respectively.

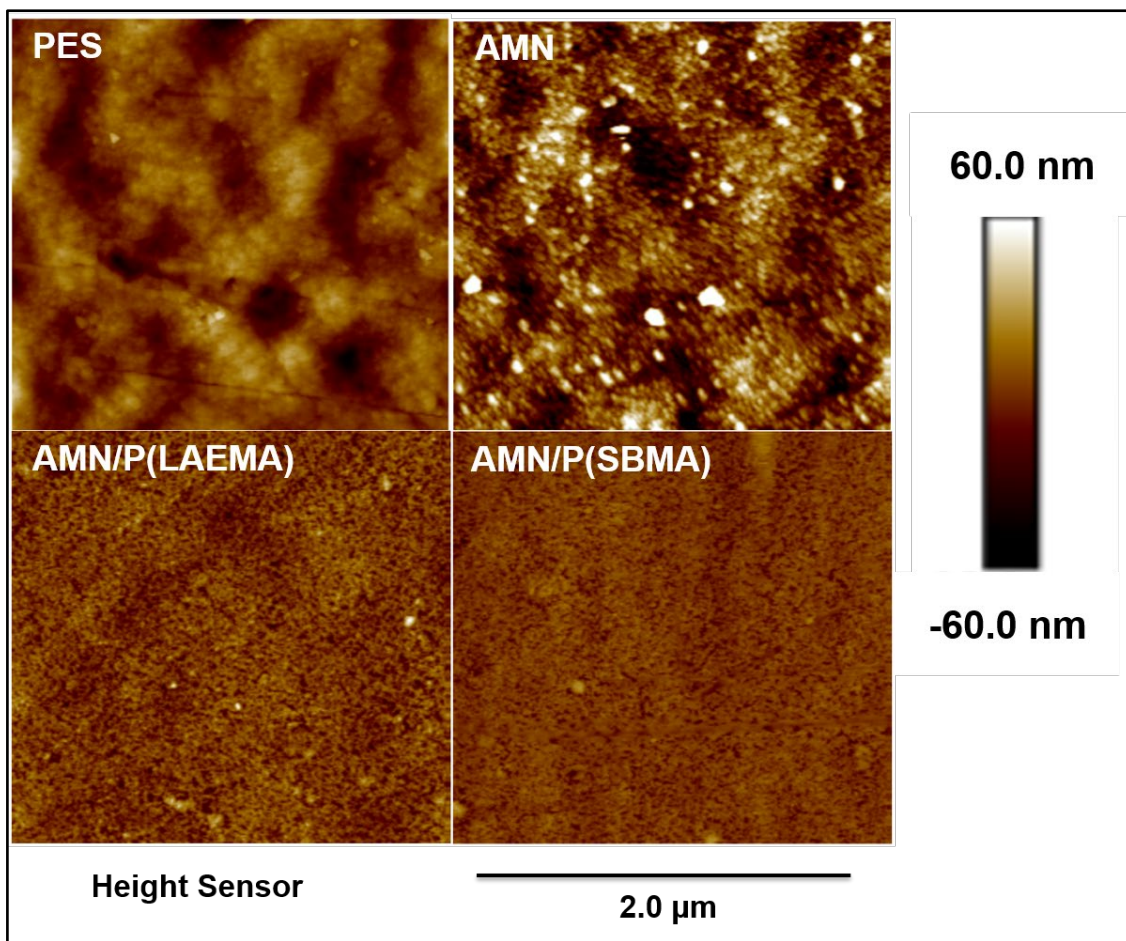


Figure 3.12. Two-dimensional topographical AFM images of the modified and unmodified membranes.

Sample	Contact Angle (°)	Surface Roughness (nm)	
		Ra	Rq
PES	77.9	12.3	9.82
AMN	41.4	19.3	15.0
AMN/P(LAEMA)	22.2	5.99	7.65
AMN/P(SBMA)	13.3	4.05	5.27

Table 3.3. Contact angle and surface roughness parameters of the modified and unmodified membranes.

3.3.4. Static Protein Adsorption tests

Membrane fouling due to non-specific adsorption of protein is strongly influenced by the physical and chemical characteristics of the membrane. The adsorption of proteins on the membrane surface results in a sharp decline in permeate flux due to the blockage of pores. Additionally, membrane fouling is also said to facilitate bacterial adhesion to surfaces as bacteria adhere to the surfaces through various mechanisms such as bio-specific and non-bio-specific adhesion. Hence it would be reasonable to hypothesize that surfaces that resist protein

adsorption would also prevent the occurrence of bacterial adhesion [87, 89]. In this study, bovine serum albumin (BSA) was used as a model protein to evaluate the antifouling ability of the membrane surfaces. BSA is highly stable, water soluble and available at high purity due to which it is commonly used as a model foulant for attachment studies. Also, at a neutral pH, BSA is negatively charged, and under acidic conditions, it is positively charged [90].

As shown in **Figure 3.13**, the pristine PES membrane had a high amount of protein adsorbed onto its surface. This could be due to the hydrophobic-hydrophobic interactions between the hydrophobic parts of BSA and the hydrophobic surface of the PES membrane. For the membrane modified with AMN, an increase in the protein adsorption was observed which could be attributed to the presence of a primary amine ($-NH_2$) functional group in AMN [80]. Primary amines are positively charged at neutral pH, while BSA is negatively charged. Hence the higher protein adsorption, could be due to the electrostatic interactions between the positively charged AMN surface, and the negatively charged BSA. After the deposition of P(LAEMA) and P(SBMA), a decrease in the protein adsorption amounts was observed. This could be attributed to the membrane hydrophilicity (as shown in table 3.3) and their excellent hydration capacity.

Furthermore, when compared to the pure PES membrane, we observed more than 20% reduction in protein adsorption in the case of membranes modified with P(LAEMA) and P(SBMA). However, there was still a significant amount protein adsorption on the surfaces of the modified membranes as can be seen in **Figure 3.13**. Hence the results need further validation by performing the surface charge analysis for the filtration membranes and the protein rejection studies via filtration tests.

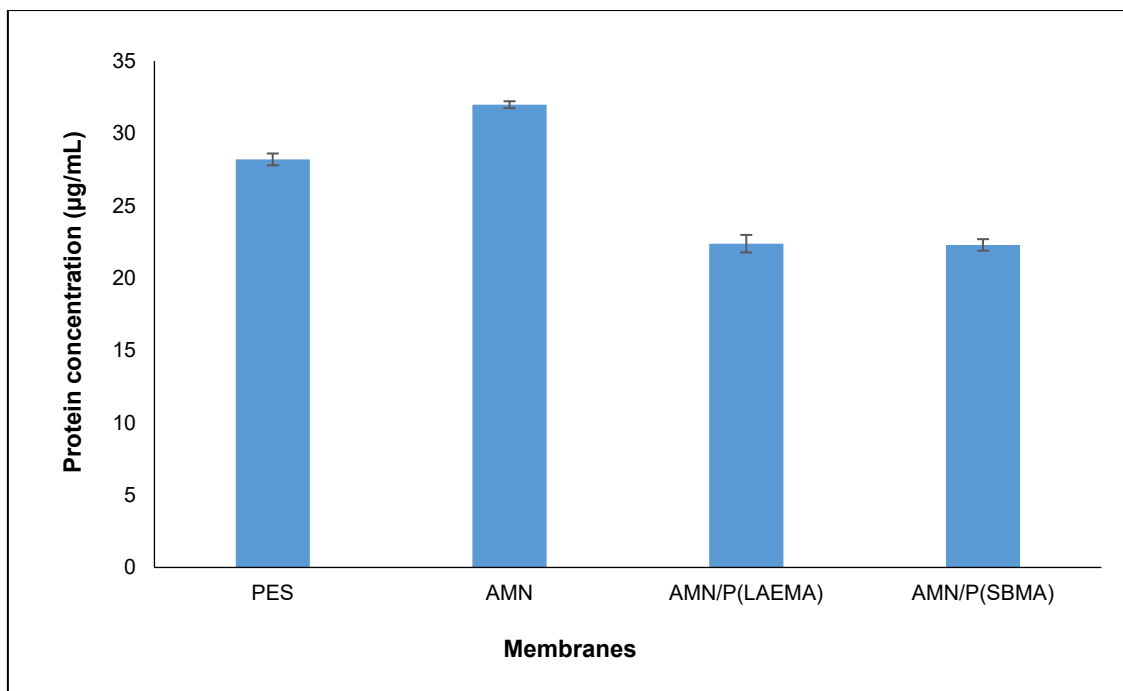


Figure 3.13. Static protein adhesion tests on the modified and unmodified membrane surfaces.

3.3.5. Surface Morphology of the Membranes after Fouling

The surface morphology of the membranes after fouling with BSA were determined using SEM. As shown in **Figure 3.14**, the fouled PES membrane displayed large aggregates of BSA despite washing the membrane with both PBS and DI water. Similarly, the membrane modified with AMN also displayed BSA particles after rinsing with both PBS and DI water. The reason behind this is attributed to the surface roughness of the membrane. However, the surfaces of the modified membranes after the deposition of P(LAEMA) and P(SBMA) were both smooth and hydrophilic as a result of which no BSA particles were visible on these surfaces.

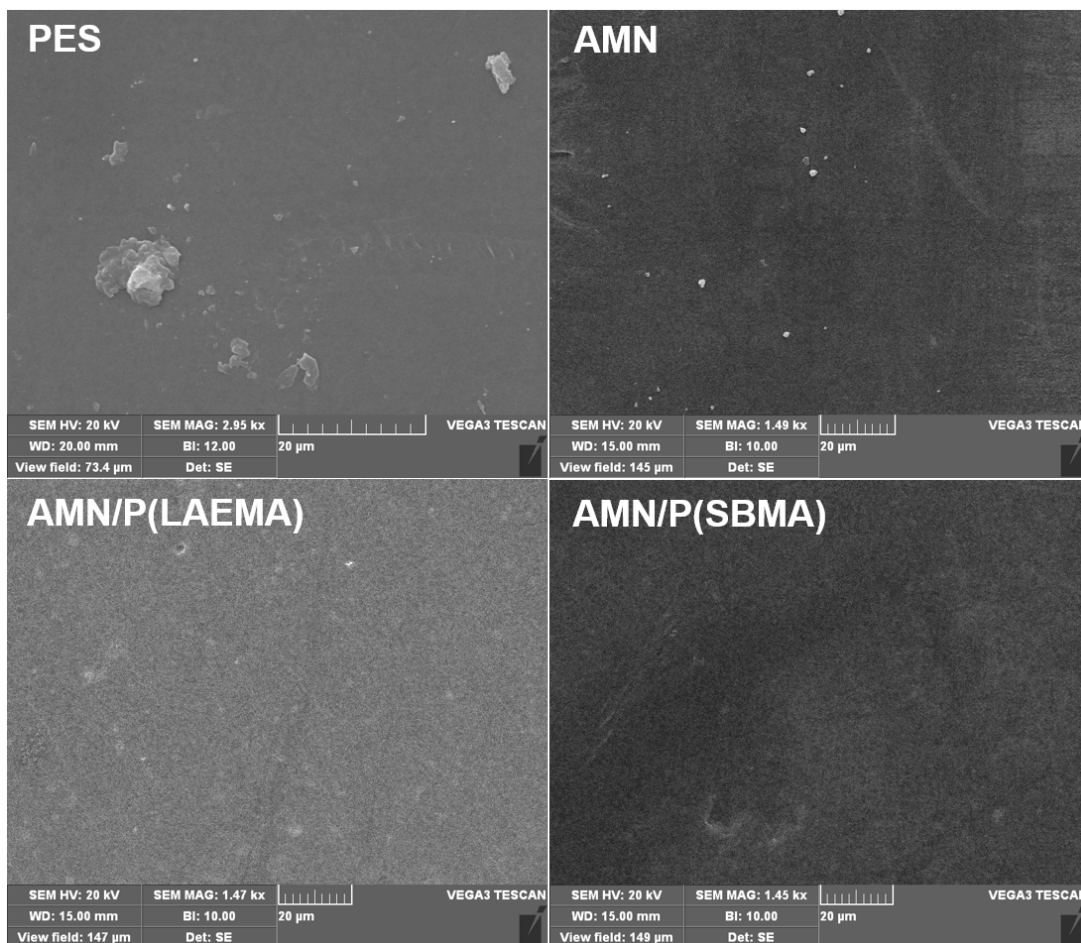


Figure 3.14. SEM images of the modified and unmodified membranes after fouling with BSA.

3.3.6. Antibacterial Activity of the Membranes

The attachment of microbial cells to surfaces depends on several factors such as van der Waals forces, surface charge, surface energy and the surface chemistry of the substrate. These cells eventually lead to the formation of biofilms comprised of a consortia of microbial cells that secrete extracellular polymeric substances (EPS). The attachment of these cells results in the blockage of pores on the membranes further resulting in flux decline [91, 92]. Hence, the antibacterial activity of the filtration membranes was evaluated against both Gram negative (*E. coli*) and Gram positive (*S. aureus*). As shown in **Figure 3.15**, the modified membranes that were incorporated with AgNPs demonstrated an excellent antibacterial activity. A clear halo zone was formed around these membranes indicating a significant inhibition effect towards both *E. coli* and *S. aureus*. This could be due to the release of Ag^+ ions into the surrounding

medium resulting in the binding of these ions with the bacterial cell membrane eventually resulting in its disruption. Silver nanoparticles (AgNPs) store and release silver ions (Ag⁺) which produce free radicals resulting in the activation of reactive oxygen species (ROS). Thus, when these Ag⁺ ions come in contact with bacteria, they penetrate and rupture the bacterial cell wall, and interrupt the reproduction of the cell DNA thereby preventing their growth [93, 94].

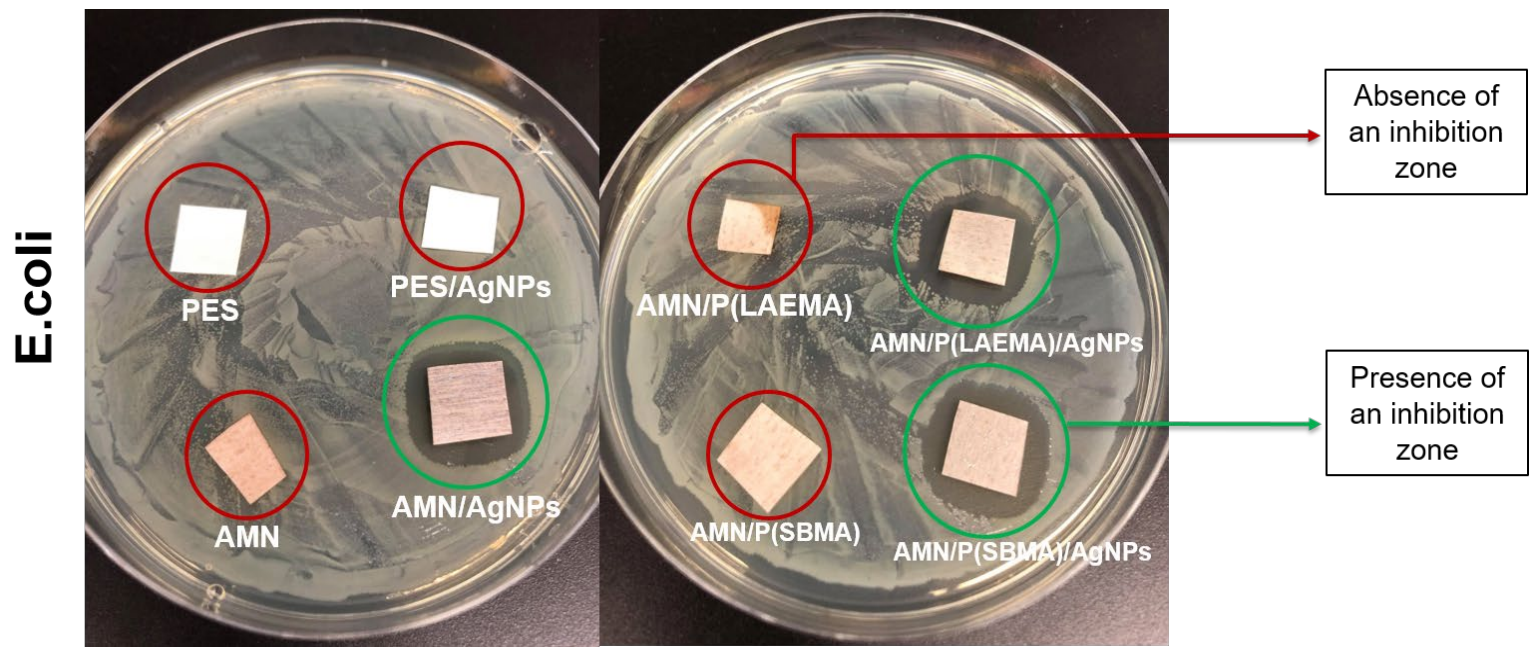


Figure 3.15 (a). Inhibition zone images of both modified and unmodified membranes against gram negative (*E.coli*) before and after their incorporation with AgNPs.

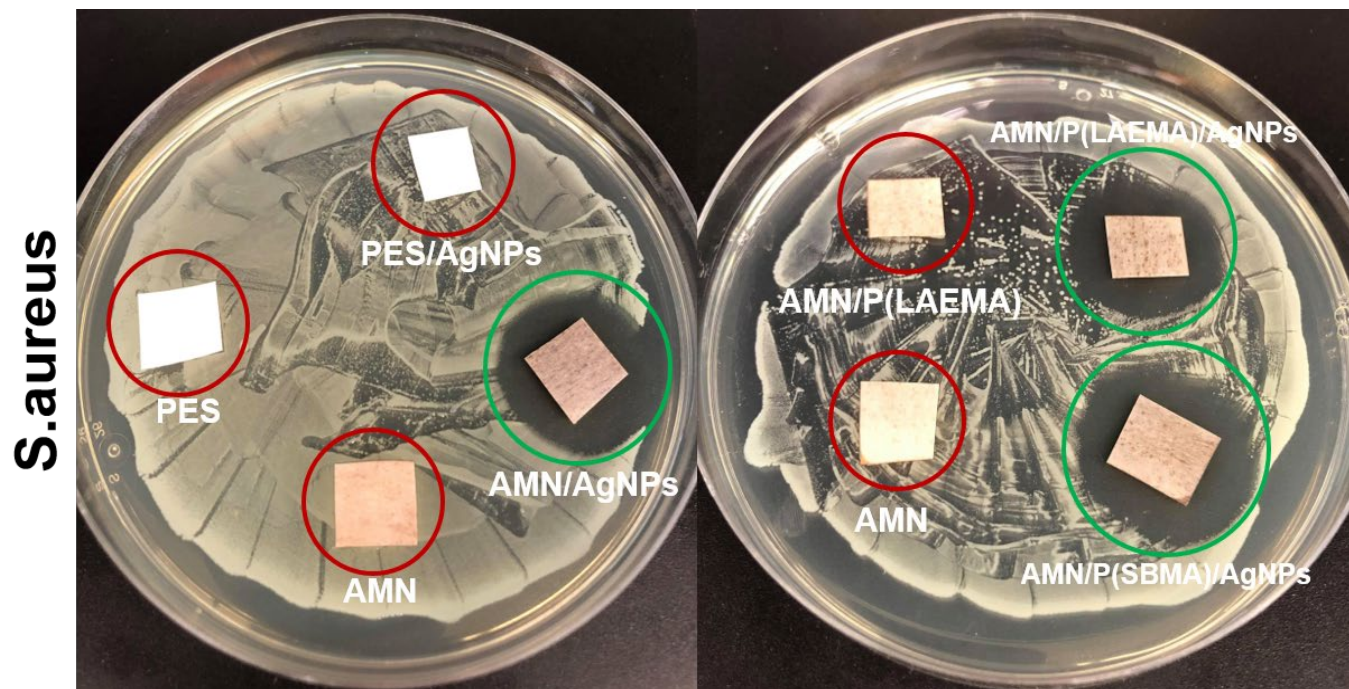


Figure 3.15 (b). Inhibition zone images of both modified and unmodified membranes against gram positive (*S. aureus*) before and after their incorporation with AgNPs.

CHAPTER 4: CONCLUSION AND FUTURE WORK

4.1. Conclusion

In this project, we successfully fabricated antifouling and antibacterial membrane surfaces using the prebiotic chemistry approach. The surface of the membrane was first modified using AMN, where the polymerization of AMN occurred due to its pH induced neutralization. The hydrophilicity of the membrane was further improved by the sequential deposition of the two polymers, (i) P(LAEMA) and (ii) P(SBMA). The two polymers were synthesized using the RAFT polymerization mechanism. The introduction of these two polymers converted the surface of the intrinsically hydrophobic PES membrane into a functional hydrophilic surface. The surface of the membrane was further loaded with AgNPs to inhibit bacterial growth and reduce bacterial adhesion on the membrane surface.

The XPS results demonstrated the successful modification of the membrane surface with AMN, and also the deposition of both the polymers. The WCA measurements showed a decrease in the contact angle after the introduction of P(LAEMA) and P(SBMA). The AFM results demonstrated an increased surface roughness of the membrane surface after its modification with AMN, which could be due to the precipitation of the polymer while surface coating. However, after the introduction of the two polymers, the membrane surface demonstrated a decrease in the surface roughness. The static protein adsorption tests also showed a highest increase in the adsorption of protein on the surface of membrane modified with AMN, which is due to its increased surface roughness. However, the introduction of the two polymers resulted in the decrease in the protein adsorption on the membrane surfaces. The antibacterial activity of the modified membranes after the deposition of AgNPs on the membrane surface showed an excellent inhibition towards both gram positive (*S. aureus*) and gram negative (*E. coli*).

From the results, we could confirm that AMN can be used as a precursor to graft compounds containing amine, nitrile, and hydroxyl functional groups. The tendency of AMN to self-polymerise under oxidative or non-oxidative conditions, in aqueous or non-aqueous solutions and in gaseous phase on various substrates makes it an interesting material of choice for surface modification applications. Furthermore, previous studies have also highlighted the

potential of prebiotic chemistry inspired coatings in biomedical applications. Thus, we conclude by saying that the prebiotic-chemistry based surface modification approach shows great potential to be utilized in modifying the surfaces of different polymeric substrates to enhance their antifouling and antibacterial properties.

4.2. Future Work

The natural organic matter (NOM) in wastewater consists of both hydrophobic and hydrophilic foulants that can lead to membrane fouling and flux decline. Also, while determining the antifouling ability of the membrane surfaces, there are also other factors that could come into play such as (i) surface charge of the membrane, and (ii) pH of the solution. The surface modification of the porous filtration membranes can result in the decrease in pore sizes, thereby resulting in a decline in pure water flux of the membranes. Thus, the studies performed in **Chapter 3** could be further extended by performing the following:

- Determining the filtration efficiency of the membranes via the pure water flux measurements using the dead-end filtration set-up for both the modified and unmodified membranes.
- Evaluate the BSA rejection and flux recovery ratios of the membranes using the dead-end filtration set-up for both the modified and unmodified membranes.
- Evaluate the surface charge of the membrane surfaces and perform the BSA rejection studies and static protein adsorption tests by under different pH conditions of the BSA solution from pH 4.0 to pH 10.0.
- Fabricate a thermo-responsive dual-functional (antifouling and antibacterial) membrane surface via the prebiotic-chemistry approach.

BIBLIOGRAPHY

1. Adeleye, A. S., Conway, J. R., Garner, K., Huang, Y., Su, Y., & Keller, A. A. (2016). Engineered nanomaterials for water treatment and remediation: Costs, benefits, and applicability. *Chemical Engineering Journal*, 286, 640-662.
2. Nqombolo, A., Mpupa, A., Moutloali, R. M., & Nomngongo, P. N. (2018). Wastewater treatment using membrane technology. *Wastewater and Water Quality*, 29.
3. Zhang, R., Liu, Y., He, M., Su, Y., Zhao, X., Elimelech, M., & Jiang, Z. (2016). Antifouling membranes for sustainable water purification: strategies and mechanisms. *Chemical Society Reviews*, 45(21), 5888-5924.
4. Karkooti, A., Rastgar, M., Nazemifard, N., & Sadrzadeh, M. (2020). Graphene-based electro-conductive anti-fouling membranes for the treatment of oil sands produced water. *Science of the Total Environment*, 704, 135365.
5. Fane, A. T., Wang, R., & Jia, Y. (2011). Membrane technology: past, present and future. In *Membrane and Desalination Technologies* (pp. 1-45). Humana Press, Totowa, NJ.
6. Lenntech.com. *Membrane technology*. [online] Available at: <https://www.lenntech.com/membrane-technology>. [Accessed 25 Feb. 2020].
7. Hofs, B., Ogier, J., Vries, D., Beerendonk, E. F., & Cornelissen, E. R. (2011). Comparison of ceramic and polymeric membrane permeability and fouling using surface water. *Separation and Purification Technology*, 79(3), 365-374.
8. Giwa, A., Ahmed, M., & Hasan, S. W. (2019). Polymers for Membrane Filtration in Water Purification. In *Polymeric Materials for Clean Water* (pp. 167-190). Springer, Cham.
9. Sadr, S. M., & Saroj, D. P. (2015). Membrane technologies for municipal wastewater treatment. In *Advances in membrane technologies for water treatment* (pp. 443-463). Woodhead Publishing.
10. Nady, N., Franssen, M. C., Zuilhof, H., Eldin, M. S. M., Boom, R., & Schroën, K. (2011). Modification methods for poly (arylsulfone) membranes: A mini review focusing on surface modification. *Desalination*, 275(1-3), 1-9.
11. Choo, K. H., & Lee, C. H. (2000). Understanding membrane fouling in terms of surface free energy changes. *Journal of colloid and interface science*, 226(2), 367-370.

12. Hilal, N., Khayet, M., & Wright, C. J. (2016). *Membrane modification: Technology and applications*. CRC press.
13. Le-Clech P. (2014) Protein Fouling. In: Drioli E., Giorno L. (eds) *Encyclopedia of Membranes*. Springer, Berlin, Heidelberg
14. Kujundzic, E., Greenberg, A. R., Fong, R., & Hernandez, M. (2011). Monitoring protein fouling on polymeric membranes using ultrasonic frequency-domain reflectometry. *Membranes*, 1(3), 195-216.
15. Khulbe, K. C., Feng, C., & Matsuura, T. (2010). The art of surface modification of synthetic polymeric membranes. *Journal of Applied Polymer Science*, 115(2), 855-895.
16. Harvesting Microalgae with Ultrafiltration Membranes. [online] Available at: <https://sites.google.com/site/algaeultrafiltration>. [Accessed 16 May 2020].
17. Chen, Y., Dong, B. Z., Gao, N. Y., & Fan, J. C. (2007). Effect of coagulation pretreatment on fouling of an ultrafiltration membrane. *Desalination*, 204(1-3), 181-188.
18. Yin, Z., Wen, T., Li, Y., Li, A., & Long, C. (2020). Alleviating reverse osmosis membrane fouling caused by biopolymers using pre-ozonation. *Journal of Membrane Science*, 595, 117546.
19. Suzuki, T., Watanabe, Y., & Ozawa, G. (2001). Performance of a hybrid MF membrane system combining activated carbon adsorption and biological oxidation. *Water Science and Technology: Water Supply*, 1(5-6), 253-259.
20. Lateef, S. K., Soh, B. Z., & Kimura, K. (2013). Direct membrane filtration of municipal wastewater with chemically enhanced backwash for recovery of organic matter. *Bioresource technology*, 150, 149-155.
21. Al-Ghamdi, M. A., Alhadidi, A., & Ghaffour, N. (2019). Membrane backwash cleaning using CO₂ nucleation. *Water research*, 165, 114985.
22. Nady, N., El-Shazly, A. H., Soliman, H., & Kandil, S. H. (2016). Protein-Repellence PES Membranes Using Bio-grafting of Ortho-aminophenol. *Polymers*, 8(8), 306.
23. Zabihi, Z., Homayoonfal, M., & Davar, F. (2020). Application of UV irradiation enhanced by CuS photosensitive nanoparticles to mitigate polysulfone membrane fouling. *Journal of Photochemistry and Photobiology A: Chemistry*, 390, 112304.

24. Vatanpour, V., Esmaeili, M., Safarpour, M., Ghadimi, A., & Adabi, J. (2019). Synergistic effect of carboxylated-MWCNTs on the performance of acrylic acid UV-grafted polyamide nanofiltration membranes. *Reactive and Functional Polymers*, 134, 74-84.
25. Wang, D., Zou, W., Li, L., Wei, Q., Sun, S., & Zhao, C. (2011). Preparation and characterization of functional carboxylic polyethersulfone membrane. *Journal of membrane science*, 374(1-2), 93-101.
26. Sabatini, V., Checchia, S., Farina, H., & Ortenzi, M. A. (2016). Homogeneous synthesis and characterization of sulfonated polyarylethersulfones having low degree of sulfonation and highly hydrophilic behavior. *Macromolecular Research*, 24(9), 800-810.
27. Haider, M. S., Shao, G. N., Imran, S. M., Park, S. S., Abbas, N., Tahir, M. S., ... & Kim, H. T. (2016). Aminated polyethersulfone-silver nanoparticles (AgNPs-APES) composite membranes with controlled silver ion release for antibacterial and water treatment applications. *Materials Science and Engineering: C*, 62, 732-745.
28. Kim, K. J., Fane, A. G., & Fell, C. J. D. (1989). The effect of Langmuir-Blodgett layer pretreatment on the performance of ultrafiltration membranes. *Journal of membrane science*, 43(2-3), 187-204.
29. Xue, J., Zhao, W., Nie, S., Sun, S., & Zhao, C. (2013). Blood compatibility of polyethersulfone membrane by blending a sulfated derivative of chitosan. *Carbohydrate polymers*, 95(1), 64-71.
30. Huang, R., Liu, Z., Yan, B., Li, Y., Li, H., Liu, D., Wang, P., Cui, F. & Shi, W. (2020). Layer-by-layer assembly of high negatively charged polycarbonate membranes with robust antifouling property for microalgae harvesting. *Journal of Membrane Science*, 595, 117488.
31. Alenazi, N. A., Hussein, M. A., Alamry, K. A., & Asiri, A. M. (2017). Modified polyether-sulfone membrane: a mini review. *Designed monomers and polymers*, 20(1), 532-546.
32. Lee, H., Dellatore, S. M., Miller, W. M., & Messersmith, P. B. (2007). Mussel-inspired surface chemistry for multifunctional coatings. *Science*, 318(5849), 426-430.

33. Van der Bruggen, B. (2009). Chemical modification of polyethersulfone nanofiltration membranes: a review. *Journal of Applied Polymer Science*, 114(1), 630-642.
34. Chen, S., Li, L., Zhao, C., & Zheng, J. (2010). Surface hydration: Principles and applications toward low-fouling/nonfouling biomaterials. *Polymer*, 51(23), 5283-5293.
35. Shakharamipour, N., Tran, T. N., Ramanan, S., & Lin, H. (2017). Membranes with surface-enhanced antifouling properties for water purification. *Membranes*, 7(1), 13.
36. Lee, H., Dellatore, S. M., Miller, W. M., & Messersmith, P. B. (2007). Mussel-inspired surface chemistry for multifunctional coatings. *Science*, 318(5849), 426-430.
37. McCloskey, B. D., Park, H. B., Ju, H., Rowe, B. W., Miller, D. J., Chun, B. J., ... & Freeman, B. D. (2010). Influence of polydopamine deposition conditions on pure water flux and foulant adhesion resistance of reverse osmosis, ultrafiltration, and microfiltration membranes. *Polymer*, 51(15), 3472-3485.
38. McCloskey, B. D., Park, H. B., Ju, H., Rowe, B. W., Miller, D. J., & Freeman, B. D. (2012). A bioinspired fouling-resistant surface modification for water purification membranes. *Journal of membrane science*, 413, 82-90.
39. Miller, S. L. (1953). A production of amino acids under possible primitive earth conditions. *Science*, 117(3046), 528-529.
40. Bada, J. L., & Lazcano, A. (2003). Prebiotic soup--revisiting the miller experiment. *Science*, 300(5620), 745-746.
41. Menzies, D. J., Ang, A., Thissen, H., & Evans, R. A. (2017). Adhesive prebiotic chemistry inspired coatings for bone contacting applications. *ACS Biomaterials Science & Engineering*, 3(5), 793-806.
42. H. Thissen *et al.*, "Prebiotic-chemistry inspired polymer coatings for biomedical and material science applications," vol. 7, no. 11, pp. e225-9, 2015.
43. Matyjaszewski, K., & Spanswick, J. (2005). Controlled/living radical polymerization. *Materials Today*, 8(3), 26-33.
44. OLenick, T. (2008). Free vs. Controlled Radical Polymerization. Retrieved 10 June 2020, from <https://www.cosmeticsandtoiletries.com/research/methodsprocesses/6469797.html>.
45. Grajales, S. Controlled Radical Materials Science Polymerization Guide. Retrieved 10 June 2020, from <https://www.sigmaaldrich.com/content/dam/sigma->

- [aldrich/docs/SAJ/Brochure/1/controlled-radical-polymerization-guide.pdf](#).
46. Perrier, S. (2017). 50th Anniversary Perspective: RAFT Polymerization □ A User Guide. *Macromolecules*, 50(19), 7433-7447.
 47. Keddie, D. J. (2014). A guide to the synthesis of block copolymers using reversible-addition fragmentation chain transfer (RAFT) polymerization. *Chemical Society Reviews*, pp. 496-505.
 48. Grinberg, N., & Rodriguez, S. (Editors). (2019). *Ewing's Analytical Instrumentation Handbook*. CRC Press.
 49. Hoffman, R. What is NMR? Retrieved 23 January 2020, from <http://chem.ch.huji.ac.il/nmr/whatisnmr/whatisnmr.html>.
 50. Quan, S. (2016). Galactose-Decorated Polymers and Nanogels Synthesized via Reversible Addition-Fragmentation Chain Transfer Polymerization for in vitro Tumor Targeted Drug Delivery and Gene Knockdown.
 51. Nanosurf.com. (n.d.). *AFM Modes and Theory — An Overview - Nanosurf*. Available at: <https://www.nanosurf.com/en/how-afm-works>. [Accessed 14 Jan. 2020].
 52. Atomic Force Microscopy Systems | AFM System | Park Systems. Retrieved 23 January 2020. Available at: <https://parksystems.com/medias/nano-academy/how-afm-works>.
 53. Qiang Li, H. (1997). AFM Scanning Modes. Retrieved 23 January 2020, from <http://www.chembio.uoguelph.ca/educmat/chm729/afm/details.htm#summary>
 54. Wei, Q. (Editor). (2009). Surface modification of textiles. *Elsevier*.
 55. Thermo Scientific XPS: What is XPS. Retrieved 23 January 2020, Available at: <https://xpssimplified.com/whatisxps.php>.
 56. Techniques. *Scanning Electron Microscopy (SEM)*. [online] Available at: https://serc.carleton.edu/research_education/geochemsheets/techniques/SEM.html. [Accessed 26 March 2020].
 57. Nanoscience Instruments. *Scanning Electron Microscopy - Nanoscience Instruments*. [online] Available at: <https://www.nanoscience.com/techniques/scanning-electron-microscopy>. [Accessed 26 March 2020].
 58. Kaech, A. (2002). An introduction to electron microscopy instrumentation, imaging and preparation. *Cent. Microsc. Image Anal*, 1-26.

59. Scanning Electron Microscopy - Nanoscience Instruments. Retrieved 31 March 2020, from <https://www.nanoscience.com/techniques/scanning-electron-microscopy>.
60. Drioli, E., Criscuoli, A., & Curcio, E. (2011). Membrane contactors: fundamentals, applications and potentialities. *Elsevier*.
61. Contact angle. Retrieved 23 January 2020, from <https://www.kruss-scientific.com/services/education-theory/glossary/contact-angle>
62. Choudhary, A. (2017). The principle of Ultra Violet (UV) Spectrophotometer. *Medium. com*.
63. N. Shahkaramipour, T. N. Tran, S. Ramanan, and H. Lin, “Membranes with Surface-Enhanced Antifouling Properties for Water Purification,” pp. 1–19, 2017.
64. S. Zhongyi, “As featured in : purification : strategies and mechanisms,” *Chem. Soc. Rev.*, vol. 45, pp. 5888–5924, 2016.
65. D. J. Miller, D. R. Dreyer, C. W. Bielawski, D. R. Paul, and B. D. Freeman, “Surface Modification of Water Purification Membranes Angewandte,” pp. 4662–4711, 2017.
66. A. Rahimpour and S. S. Madaeni, “Polyethersulfone (PES)/ cellulose acetate phthalate (CAP) blend ultrafiltration membranes : Preparation, morphology, performance and antifouling properties,” vol. 305, pp. 299–312, 2007.
67. J. Lin *et al.*, “Chemical Engineering and Processing : Process Intensification Enhancement of polyethersulfone (PES) membrane doped by monodisperse Stöber silica for water treatment,” *Chem. Eng. Process. Process Intensif.*, vol. 107, pp. 194–205, 2016.
68. D. Rana and T. Matsuura, “Surface Modifications for Antifouling Membranes,” pp. 2448–2471, 2010.
69. N. Nady, A. H. El-shazly, H. M. A. Soliman, and S. H. Kandil, “Bio-grafting of Ortho-aminophenol.”
70. F. Li, J. Meng, J. Ye, B. Yang, Q. Tian, and C. Deng, “Surface modification of PES ultrafiltration membrane by polydopamine coating and poly (ethylene glycol) grafting : Morphology, stability, and anti-fouling,” *DES*, vol. 344, pp. 422–430, 2014.
71. S. F. Hvid KB, Nielsen PS, “Preparation and characterization of a new ultrafiltration membrane,” *J. Memb. Sci.*, vol. 53, no. 3, pp. 189–202, 1990.
72. Gancarz, I., Poźniak, G., & Bryjak, M. (2000). Modification of polysulfone

- membranes: 3. Effect of nitrogen plasma. *European Polymer Journal*, 36(8), 1563-1569.
73. X. Qiao, Z. Zhang, and Z. Ping, "Hydrophilic modification of ultrafiltration membranes and their application in *Salvia Miltiorrhiza* decoction," vol. 56, pp. 265–269, 2007.
74. R. Kou, Z. Xu, H. Deng, Z. Liu, P. Seta, and Y. Xu, "Surface Modification of Microporous Polypropylene Membranes by Plasma-Induced Graft Polymerization of *r*-Allyl Glucoside," no. 19, pp. 6869–6875, 2003.
75. T. Gullinkala and I. Escobar, "Study of the Hydrophilic- Enhanced Ultrafiltration Membrane," vol. 27, no. 2, 2008.
76. Lee, H., Dellatore, S. M., Miller, W. M., & Messersmith, P. B. (2007). Mussel-inspired surface chemistry for multifunctional coatings. *science*, 318(5849), 426-430.
77. L. Tang, K. J. T. Livi, and K. L. Chen, "Polysulfone membranes modified with bioinspired polydopamine and silver nanoparticles formed in situ to mitigate biofouling," *Environ. Sci. Technol. Lett.*, vol. 2, no. 3, pp. 59–65, 2015.
78. Reis, R. L., Neves, N. M., Mano, J. F., Gomes, M. E., Marques, A. P., & Azevedo, H. S. (2008). *Natural-based polymers for biomedical applications*. Elsevier.
79. A. K. Helmut Thissen, Richard Evans, "Hydrogen cyanide-based polymer surface coatings and hydrogels," 2013.
80. Thissen, H., Koegler, A., Salwiczek, M., Easton, C. D., Qu, Y., Lithgow, T., & Evans, R. A. (2015). Prebiotic-chemistry inspired polymer coatings for biomedical and material science applications. *NPG Asia Materials*, 7(11), e225-e225.
81. Menzies, D. J., Ang, A., Thissen, H., & Evans, R. A. (2017). Adhesive prebiotic chemistry inspired coatings for bone contacting applications. *ACS Biomaterials Science & Engineering*, 3(5), 793-806.
82. Ahmed, M., & Narain, R. (2012). Intracellular delivery of DNA and enzyme in active form using degradable carbohydrate-based nanogels. *Molecular pharmaceuticals*, 9(11), 3160-3170.
83. Deng, Z., Li, S., Jiang, X., & Narain, R. (2009). Well-defined galactose-containing multi-functional copolymers and glyconanoparticles for biomolecular recognition processes. *Macromolecules*, 42(17), 6393-6405.

84. N. Shahkaramipour, C. K. Lai, S. R. Venna, H. Sun, C. Cheng, and H. Lin, "Membrane Surface Modification Using Thiol-Containing Zwitterionic Polymers via Bioadhesive Polydopamine," 2018.
85. Xie, Y., Li, S. S., Jiang, X., Xiang, T., Wang, R., & Zhao, C. S. (2015). Zwitterionic glycosyl modified polyethersulfone membranes with enhanced anti-fouling property and blood compatibility. *Journal of colloid and interface science*, 443, 36-44.
86. Asha, A. B., Chen, Y., Zhang, H., Ghaemi, S., Ishihara, K., Liu, Y., & Narain, R. (2018). Rapid Mussel-Inspired Surface Zwitteration for Enhanced Antifouling and Antibacterial Properties. *Langmuir*, 35(5), 1621-1630.
87. Xie, Y., Tang, C., Wang, Z., Xu, Y., Zhao, W., Sun, S., & Zhao, C. (2017). Co-deposition towards mussel-inspired antifouling and antibacterial membranes by using zwitterionic polymers and silver nanoparticles. *Journal of Materials Chemistry B*, 5(34), 7186-7193.
88. Thapa, B., Kumar, P., Zeng, H., & Narain, R. (2015). Asialoglycoprotein receptor-mediated gene delivery to hepatocytes using galactosylated polymers. *Biomacromolecules*, 16(9), 3008-3020.
89. Doncom, K. E., Warren, N. J., & Armes, S. P. (2015). Polysulfobetaine-based diblock copolymer nano-objects via polymerization-induced self-assembly. *Polymer Chemistry*, 6(41), 7264-7273.
90. Zhu, L. P., Zhang, X. X., Xu, L., Du, C. H., Zhu, B. K., & Xu, Y. Y. (2007). Improved protein-adsorption resistance of polyethersulfone membranes via surface segregation of ultrahigh molecular weight poly (styrene-alt-maleic anhydride). *Colloids and Surfaces B: Biointerfaces*, 57(2), 189-197.
91. Bao, Q., Xie, L., Ohashi, H., Hosomi, M., & Terada, A. (2019). Inhibition of *Agrobacterium tumefaciens* biofilm formation by acylase I-immobilized polymer surface grafting of a zwitterionic group-containing polymer brush. *Biochemical Engineering Journal*, 152, 107372.
92. Gafri, H. F. S., Zuki, F. M., Aroua, M. K., & Hashim, N. A. (2019). Mechanism of bacterial adhesion on ultrafiltration membrane modified by natural antimicrobial polymers (chitosan) and combination with activated carbon (PAC). *Reviews in Chemical Engineering*, 35(3), 421-443.

93. Sile-Yuksel, M., Tas, B., Koseoglu-Imer, D. Y., & Koyuncu, I. (2014). Effect of silver nanoparticle (AgNP) location in nanocomposite membrane matrix fabricated with different polymer type on antibacterial mechanism. *Desalination*, *347*, 120-130.
94. Maziya, K., Dlamini, B. C., & Malinga, S. P. (2020). Hyperbranched polymer nanofibrous membrane grafted with silver nanoparticles for dual antifouling and antibacterial properties against *Escherichia coli*, *Staphylococcus aureus* and *Pseudomonas aeruginosa*. *Reactive and Functional Polymers*, *148*, 104494.